Effects of Biological Oxidants on the Catalytic Activity and Structure of Group VIA Phospholipase A_2[†]

Haowei Song, Shunzhong Bao, Sasanka Ramanadham, and John Turk*

Medicine Department Mass Spectrometry Facility, Division of Endocrinology, Metabolism, and Lipid Research, Washington University School of Medicine, St. Louis, Missouri 63110

Received March 13, 2006; Revised Manuscript Received March 28, 2006

ABSTRACT: Group VIA phospholipase A_2 (iPLA$_2\beta$) is expressed in phagocytes, vascular cells, pancreatic islet β-cells, neurons, and other cells and plays roles in transcriptional regulation, cell proliferation, apoptosis, secretion, and other events. A bromoenol lactone (BEL) suicide substrate used to study iPLA$_2\beta$ functions inactivates iPLA$_2\beta$ by alkylating Cys thiols. Because thiol redox reactions are important in signaling and some cells that express iPLA$_2\beta$ produce biological oxidants, iPLA$_2\beta$ might be subject to redox regulation. We report that biological concentrations of H_2O_2, NO, and HOCl inactivate iPLA$_2\beta$, and this can be partially reversed by dithiothreitol (DTT). Oxidant-treated iPLA$_2\beta$ modifications were studied by LC−MS/MS analyses of tryptic digests and included DTT-reversible events, e.g., formation of disulfide bonds and sulfenic acids, and others not so reversed, e.g., formation of sulfonic acids, Trp oxides, and Met sulfoxides. W^{460} oxidation could cause irreversible inactivation because it is near the lipase consensus sequence (^{463}GTSTG^{467}), and site-directed mutagenesis of W^{460} yields active mutant enzymes that exhibit no DTT-irreversible oxidative inactivation. Cys651-sulfenic acid formation could be one DTT-reversible inactivation event because Cys651 modification correlates closely with activity loss and its mutagenesis reduces sensitivity to inhibition. Intermolecular disulfide bond formation might also cause reversible inactivation because oxidant-treated iPLA$_2\beta$ contains DTT-reducible oligomers, and oligomerization occurs with time- and temperature-dependent iPLA$_2\beta$ inactivation that is attenuated by DTT or ATP. Subjecting insulinoma cells to oxidative stress induces iPLA$_2\beta$ oligomerization, loss of activity, and subcellular redistribution and reduces the rate of release of arachidonate from phospholipids. These findings raise the possibility that redox reactions affect iPLA$_2\beta$ functions.

Phospholipase A_2 (PLA$_2$)[1] enzymes catalyze hydrolysis of *sn*-2 fatty acid substituents from glycerophospholipid substrates to yield a free fatty acid, e.g., arachidonic acid, and a 2-lysophospholipid that have intrinsic mediator activities and are precursors of prostaglandins, thromboxanes, leukotrienes, and platelet activating factor (PAF) (*1*−*5*). Mammalian PLA$_2$s include the PAF-acetylhydrolase family and low-molecular weight secretory PLA$_2$ (sPLA$_2$) enzymes that require millimolar Ca^{2+} concentrations for catalysis (*3*). Of group IV cytosolic PLA$_2$ (cPLA$_2$) family members (*3*), cPLA$_2\alpha$ prefers substrates with *sn*-2 arachidonoyl residues, associates with its substrates in membranes when the cytosolic Ca^{2+} concentration rises, and is also regulated by phosphorylation (*6*). Several other cPLA$_2$ family members arise from separate genes (*7*−*10*).

Group VI PLA$_2$ (iPLA$_2$) enzymes (*11*−*14*) do not require Ca^{2+} for catalysis and are inhibited by a bromoenol lactone (BEL) suicide substrate that does not inhibit sPLA$_2$ or cPLA$_2$ at similar concentrations (*15*−*18*). Group VIA PLA$_2$ (iPLA$_2\beta$) resides in the cytoplasm of resting cells, but group VIB PLA$_2$ (iPLA$_2\gamma$) contains a peroxisomal targeting sequence and is membrane-associated (*19*−*22*). These enzymes belong to a larger class of serine lipases that are encoded by multiple genes (*23*, *24*). The iPLA$_2\beta$ enzymes cloned from various species are 84−88 kDa proteins that contain a GXSXG lipase consensus sequence and eight stretches of a repetitive motif homologous to that in the protein-binding domain of ankyrin (*11*−*13*). No crystal structures of group VI PLA$_2$ family members have yet been determined.

Many potential biological functions are proposed for iPLA$_2\beta$ (*25*−*39*), and the facts that multiple splice variants are differentially expressed among cells and form hetero-oligomers with distinct properties suggest that iPLA$_2\beta$ gene products might have multiple functions depending on cellular context (*27*, *28*). Among the roles proposed for iPLA$_2\beta$ are

[†] This work was supported by U.S. Public Health Service Grants R37-DK34388, R01-69455, P01-HL57278, P41-RR00954, P60-DK20579, and P30-DK56341.

* To whom correspondence should be addressed: Washington University School of Medicine, Campus Box 8127, 660 S. Euclid Ave., St. Louis, MO 63110. Telephone: (314) 362-8190. Fax: (314) 362-7451. E-mail: jturk@wustl.edu.

[1] Abbreviations: BEL, bromoenol lactone suicide substrate; BSA, bovine serum albumin; CAD, collisionally activated dissociation; DTT, dithiothreitol; ECL, enhanced chemiluminescence; ESI, electrospray ionization; HBSS, Hank's balanced salt solution; HPLC, high-performance liquid chromatography; iPLA$_2\beta$, group VIA phospholipase A_2; IMAC, immobilized metal affinity chromatography; iNOS, inducible nitric oxide synthase; KRB, Krebs-Ringer bicarbonate buffer; LC, liquid chromatography; MEM, minimal essential medium; MPO, myeloperoxidase; MS, mass spectrometry; MS/MS, tandem mass spectrometry; NOS, nitric oxide synthase; PAGE, polyacrylamide gel electrophoresis; PLA$_2$, phospholipase A_2; Q-TOF, quadrupole time-of-flight; RT, reverse transcriptase; SD, standard deviation; SDS, sodium dodecyl sulfate.

10.1021/bi060502a CCC: $33.50
Published on Web 04/28/2006

participation in phospholipid remodeling (*25*, *26*), signaling in secretion (*29*−*31*), apoptosis (*32*, *33*), vasomotor regulation (*34*, *35*), transcriptional regulation (*36*, *37*), eicosanoid generation (*38*, *39*), and cell proliferation (*40*−*44*).

Many cells express multiple distinct PLA$_2$ enzymes (*13*, *17*, *18*, *45*), and attempts to determine their individual functions have in large part relied on pharmacologic inhibitors that discriminate among PLA$_2$s. The mechanism-based iPLA$_2$ inhibitor BEL and its enantiomers (*15*, *16*, *34*) inhibit iPLA$_2$ at concentrations lower than those required to inhibit sPLA$_2$ or cPLA$_2$ enzymes (*14*−*18*), and this has been widely exploited in discerning potential biological roles for iPLA$_2$ (*25*−*44*). BEL affects more than one target (*19*, *23*, *24*, *46*, *47*), however, and it was first developed as an inhibitor of serine proteases, e.g., chymotrypsin (*48*, *49*). BEL is a substrate for chymotrypsin (*48*, *49*) and iPLA$_2\beta$ (*15*, *16*), and its inhibitory effects require its hydrolysis by and result in covalent modifications of those enzymes (*15*, *16*, *48*, *49*). We recently demonstrated that BEL inhibits iPLA$_2\beta$ by a mechanism that involves its hydrolysis to a diffusible bromomethyl ketoacid that alkylates cysteine thiols in the enzyme (*50*). This raises the possibility that iPLA$_2\beta$ might be subject to redox regulation.

Factors that affect the oxidation state of cysteine thiols play important signaling roles in regulating transcription, the actions of growth factors and hormones, ion channel function, and other processes (*51*−*54*). Growth factors and insulin activate NADPH oxidases in some target cells to cause production of superoxide anion, which dismutates to H_2O_2, and H_2O_2 oxidizes cysteine thiols in the active sites of protein tyrosine phosphatases and lipid phosphatases to inactivate these enzymes (*55*). The iPLA$_2\beta$ inhibitor BEL also inactivates some lipid phosphatases (*46*, *47*). Inactivation of protein tyrosine phosphatases by H_2O_2 amplifies the effect of growth factor receptor tyrosine kinases to induce tyrosine phosphorylation, and this appears to be required for optimal growth factor signaling because overexpression of peroxiredoxins that catalyze reduction of H_2O_2 attenuates growth factor action (*56*−*58*).

While a role for reactive oxygen and nitrogen intermediates in inflicting cellular injury and in killing pathogenic microorganisms and tumor cells has long been recognized, many of these molecules also have signaling functions such as those described above for H_2O_2 that involve covalent modification of their targets (*59*). NO is another example of such a molecule (*59*). At the high concentrations produced by inducible NO synthase (iNOS), NO has microbicidal and tumoricidal actions, and at low concentrations produced by constitutive NOS isoforms, it plays signaling roles that often involve covalent modification of thiols (*59*). Hypochlorous acid (HOCl) is another biological oxidant produced from H_2O_2 and Cl^- by the enzyme myeloperoxidase (MPO), and it participates in microbial killing by phagocytic cells (*60*−*63*). HOCl might also have signaling functions that involve thiol modification (*64*−*70*).

At pH 7.4, HOCl and OCl^- exist in an approximately equimolar ratio, and HOCl readily traverses cell membranes to interact with intracellular targets that include glutathione and thiol enzymes, such as glyceraldehyde-3-phosphate dehydrogenase (GAPDH) (*63*−*66*). This can activate signaling cascades, such as MAP kinase pathways and the tumor suppressor p53 (*67*−*69*). In addition, MPO expression in human brain neurons and in cultured neuronal cell lines has been demonstrated, and this raises the possibility that HOCl might play a signaling role in neurons analogous to that of NO produced by neuronal NO synthase (*70*). Neurons and insulin-secreting β-cells exhibit many biochemical similarities not shared by other cells (*71*, *72*), and we find that cultured β-cells also express MPO (unpublished observations).

The influence of biological oxidants on iPLA$_2\beta$ is of interest because generation of superoxide and H_2O_2 from mitochondrial substrate overload and from tissue NADPH oxidases is thought to play a critical role in diabetic complications, including the progressive decline of β-cell function caused by hyperglycemia (*73*−*77*). iPLA$_2\beta$ is strongly expressed in β-cells and participates in insulin secretion and in β-cell proliferation and apoptosis (*30*, *31*, *33*, *41*), and effects of biological oxidants such as H_2O_2 on its activity might affect these processes. β-Cells stimulated with cytokines also produce NO via iNOS (*78*, *79*), and iPLA$_2\beta$ is required for iNOS induction in virally infected macrophages (*37*), suggesting that effects of NO on iPLA$_2\beta$ could be biologically significant. Phagocyte-derived HOCl is also believed to exert atherogenic effects on vascular endothelium (*68*, *77*), and iPLA$_2\beta$ is expressed in phagocytes (*37*), endothelium (*80*), and vascular myocytes (*43*). Both iPLA$_2\beta$ (*81*, *82*) and MPO (*70*) are also strongly expressed in brain, and effects of HOCl on iPLA$_2\beta$ could thus also be important.

We have therefore examined effects of the biological oxidants H_2O_2, NO, and HOCl on the activity of purified, recombinant iPLA$_2\beta$ and have characterized oxidant-induced covalent modifications by digesting oxidant-treated iPLA$_2\beta$ with proteases and then analyzing peptides in the digest by LC−ESI-MS/MS.

EXPERIMENTAL PROCEDURES

Materials. Spodoptera frugiperda (Sf9) cells and culture medium were purchased from Invitrogen (Carlsbad, CA). TALON metal affinity resin was from Clontech (Palo Alto, CA). [5,6,8,9,11,12,14,15-^{3}H]Arachidonic acid (217 Ci/mmol), enhanced chemiluminescence (ECL) reagents, and 1-palmitoyl-2-[^{14}C]linoleoyl-*sn*-glycero-3-phosphocholine (16:0/[^{14}C]18:2-GPC) were from Amersham Biosciences (Piscataway, NJ). Sodium dodecyl sulfate−polyacrylamide gel electrophoresis (SDS−PAGE) supplies and Coomassie Brilliant Blue stain were from Bio-Rad (Richmond, CA). Polyclonal antibodies to iPLA$_2\beta$ were obtained from Santa Cruz Biotechnology (Santa Cruz, CA). Gentamicin and INS-1 cell culture media were obtained from the Washington University Tissue Culture Support Center. The NO donor compound diethylamine NONQate and other chemicals were purchased from Sigma Chemical (St. Louis, MO). Solvents were purchased from Fisher Chemical (St. Louis, MO). PepMap HPLC columns and precolumns were obtained from LC-Packings (San Francisco, CA).

Oxidation Reactions. Stock solutions of H_2O_2, HOCl, and the NO donor compound diethylamine NONQate were prepared and calibrated as described previously (*83*). Reactions were performed at 37 °C in buffer [50 mM Na_2HPO_4 and 20 mM imidazole (pH 7.8)] containing 0.2 μg/μL iPLA$_2\beta$ with various concentrations of oxidant for various

intervals and terminated by adding a 10-fold molar excess of L-methionine.

Cloning, Expression, and Purification of Native and His-Tagged iPLA$_2\beta$ Proteins. Sf9 cells were cultured as described previously (*84*). For protein expression, cDNA encoding iPLA$_2\beta$ with a polyhistidine tag sequence at the C- or N-terminus (*84*) was cloned into the EcoRI−SalI site of pFastBac1 baculovirus shuttle vector (Invitrogen). Sf9 cell suspensions were infected with recombinant baculovirus, collected by centrifugation, and disrupted by sonication. His-tagged proteins were purified with a TALON metal affinity column, as described previously (*84*). Aliquots of protein solutions were analyzed by SDS−PAGE. Proteins were visualized by Coomassie staining or by being transferred to nylon membranes and immunoblotting, as described previously (*84*).

Assay of iPLA$_2\beta$ Enzymatic Activity. Ca^{2+}-independent PLA_2 enzymatic activity was assayed after ethanolic injection of substrate 1-palmitoyl-2-[^{14}C]linoleoyl-*sn*-glycero-3-phosphocholine into assay buffer [40 mM Tris (pH 7.5) and 5 mM EGTA] by monitoring release of [^{14}C]linoleate, as described previously (*85*).

Quantitation of Free Thiols. The amount of free thiol was measured with a thiol and sulfide quantitation kit from Molecular Probes (Eugene, OR) according to the manufacturer's instructions. In this spectrophotometric assay, thiols reduce an inactive disulfide derivative of papain (papain-S-SCH_3) and release the active enzyme (papain-SH). Activated papain catalyzes hydrolysis of the chromogenic substrate, *N*-benzoyl-L-arginine-*p*-nitroanilide (L-BAPNA), resulting in an amplified spectrophotometric signal proportional to the amount of thiol. Enzyme activity is determined by measuring the absorbance at 410 nm of the *p*-nitroaniline chromophore released from L-BAPNA on a Titertek Multiskan MCC/340 microplate reader (ICN Biomedicals, Aurora, OH). Thiol concentrations in the samples are determined from measured absorbances by interpolation from a standard curve prepared with 0.1 mM L-Cys (*50*).

LC−ESI-MS/MS Analyses. As previously described (*51*), samples (0.2 μL) were injected into a Micromass (Manchester, U.K.) CapLC liquid chromatography system and concentrated on a PepMap C18 precolumn (300 μm × 5 mm). The precolumn was then washed (3 min, 0.1% formic acid, flow rate of 30 μL/min), and the sample was eluted onto an analytical C18 column (150 mm × 17 μm) and analyzed with a solvent gradient from solution A (3% acetonitrile) to solution B (95% acetonitrile) containing 0.1% formic acid over 50 min at a flow rate reduced from 5 μL/min to 200 nL/min by stream splitting. LC eluant was introduced into the nanoflow source of a Micromass Q-TOF Micro mass spectrometer. The source temperature was 80 °C, and the cone gas flow rate was 50 L/h. A voltage of 3.2 kV was applied to the nanoflow probe tip, and data were acquired in positive ion mode. Survey scans were integrated over 1 s, and MS/MS scans were integrated over 3 s. Switching from survey to MS/MS scan mode was performed in a data-dependent manner. The maximum MS/MS-to-survey scan ratio was 3. The collision energy was 28 eV. Data were processed with Masslynx version 3.5. Multipoint calibration was performed using selected fragment ions produced by CAD of Glu-fibrino-peptide B. MS/MS spectra were processed by Masslynx software to produce a peak list file, as described previously (*84*).

Site-Directed Mutagenesis of W^{460} to T^{460} or Y^{460} To Yield His-Tagged iPLA$_2\beta$ Mutant Proteins. A 2.2 kb rat iPLA2β cDNA was subcloned into the vector pBluescript II SK (Stratagene) and used for mutagenesis. Substitution of Thr460 or Tyr460 for Trp460 was performed with the QuickChange mutagenesis kit (Stratagene, La Jolla, CA), as described previously (*50*). The sequence of the forward primer was 5′-CCAAGGACCTCTTCGACACCGTGGCAGGAACCA-GCACAG-3′ and 5′-CCAAGGACCTCTTCGACTATGTG-GCAGGAACCAGCACAG-3′. The fidelity of the construct was confirmed by sequencing, and the mutant cDNA was subcloned into the pFast-Bac1 vector, which was used to prepare recombinant baculovirus containing the mutant construct as an insert. His-tagged iPLA$_2\beta$T^{460} or iPLA$_2\beta$Y^{460} mutant protein was expressed in Sf9 cells and purified by immobilized metal affinity chromatography (IMAC), as described above.

Immunoblotting Analyses of iPLA$_2\beta$ Protein. Protein in iPLA$_2\beta$ preparations purified by IMAC after expression in an Sf9 cell-baculovirus system or proteins from INS-1 insulinoma cells that overexpress iPLA$_2\beta$ were analyzed by 8% SDS−PAGE, transferred onto Immobilon-P PVDF membranes, and processed for immunoblotting analyses. iPLA$_2\beta$ immunoreactive protein bands were visualized by enhanced chemiluminescence (ECL), as described previously (*86*).

Preparation of a Construct for Expressing iPLA$_2\beta$ as a Fusion Protein with EGFP and Selection of Stably Transfected Clones. Full-length iPLA$_2\beta$ cDNA was amplified by PCR using the following primer set: sense, 5′-AGCTTC-GAATTCATGCAGTTCTTTGGACGC-3′; and antisense, 5′-TTCGATATCGGGAGATAGCAGCAGCTGG-3′. The amplified full-length iPLA$_2\beta$ from the pMSCV-neo-iPLA$_2\beta$ constructs were then subcloned into the pEGFP-N2 vector (Clontech) after the immediate-early promoter of cytomegalovirus major and before the EGFP coding sequences in the same code-reading frame as EGFP, as described previously (*87*). The EGFP-N2 control vector and the construct encoding iPLA$_2\beta$-EGFP (FPN2) fusion protein were transfected into INS-1 cells with a Gene PORTER transfection system according to the manufacturer's instructions (Gene Therapy Systems, San Diego, CA). Stably transfected clones were selected using G418 (0.4 mg/mL). Stably transfected cells obtained with the EGFP-N2 control vector and FPN2 construct are designed as N2 cells and FPN2 cells, respectively.

Fluorescence Microscopic Analyses of the Subcellular Distribution of EGFP-Tagged iPLA$_2\beta$ in INS-1 Insulinoma Cells. The subcellular distribution of iPLA$_2\beta$ protein was visualized in INS-1 cells that expressed EGFP-tagged iPLA$_2\beta$ constructs by cytofluorescence analyses after the medium was removed and the cells were washed with PBS. Fluorescence microscopy was performed at an excitation wavelength of 550 nm and an emission wavelength of 570 nm, as previously described (*87*).

[^{3}H]Arachidonic Acid Release Measurements. INS-1 insulinoma cells (5×10^5 cells/well) were prelabeled for 20 h with [^{3}H]arachidonic acid at a final concentration of 0.5 μCi/mL (5 nM) and incubated (1 h) in serum-free medium. Cells were then washed thrice with glucose-free RPMI-1640

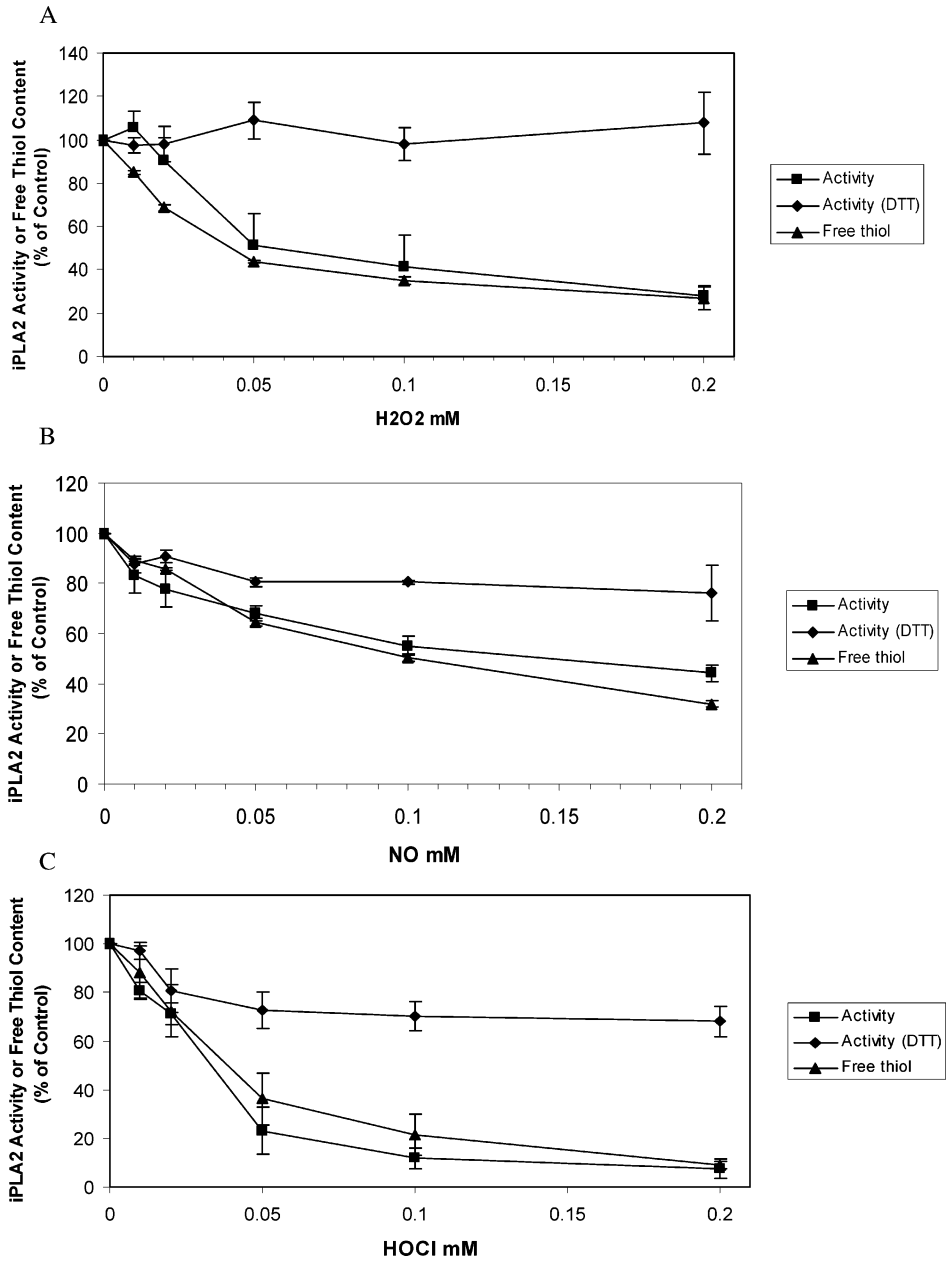

FIGURE 1: Effects of biological oxidants and dithiothreitol on the catalytic activity and thiol content of recombinant, purified group VIA phospholipase A_2 (iPLA$_2\beta$). Varied concentrations of H_2O_2 (A), the NO donor compound diethylamine NONQate (B), or HOCl (C) were added to solutions of recombinant, His-tagged iPLA$_2\beta$ (0.2 μg/mL) that had been purified by IMAC, and the mixtures were incubated at 37 °C for 30 min. The oxidation reactions were then quenched with a 10-fold molar excess of L-methionine. Aliquots of each sample were then removed for measurement of iPLA$_2\beta$ activity (■) and free thiol content (▲). A third aliquot of each sample was incubated with 2.5 mM DTT at 37 °C for 30 min, and iPLA$_2\beta$ activity was then measured (◆). Displayed values represent means ± SD ($n = 6$).

medium to remove unincorporated radiolabel. Cell viability exceeded 98% by trypan blue exclusion. Labeled cells were incubated in RPMI-1640 medium containing 0.5% BSA at 37 °C and treated with various concentrations of diamide or vehicle for various intervals, as specified in the legend of Figure 11. Supernatants and cells were separated by centrifugation (500*g* for 5 min) and assayed for ^{3}H content by liquid scintillation spectrometry, as described previously (*86*).

RESULTS

Effects of Biological Oxidants on iPLA$_2\beta$ Catalytic Activity and Cysteine Content. Affinity-purified, recombinant, His-tagged iPLA$_2\beta$ was treated with H_2O_2 at varied concentrations within the range that can be produced by cells (*88*, *89*). An H_2O_2-dependent loss of iPLA$_2\beta$ activity occurred, with ~50 and ~70% inhibition achieved at 50 and 70 μM H_2O_2, respectively, and loss of activity correlated closely with loss of free thiol groups (Figure 1A). This suggests that oxidation of cysteine thiols is involved in inactivation of iPLA$_2\beta$ by H_2O_2, and activity could be restored completely by incubating the enzyme with dithiothreitol (DTT) after treatment with H_2O_2. This suggests that reversible oxidation events, such as formation of disulfide bonds or sulfenic acids (*52*, *55*), are responsible for H_2O_2-induced inactivation of iPLA$_2\beta$.

Exposure of iPLA$_2\beta$ to NO by including various concentrations of the NO donor compound diethylamine NONQate in the incubation medium also resulted in a concentration-

1	(MO)QFFGRLVNT	LSSVTNLFSN	PFRVKEVSLA	DYASSERVRE	EGQLILLQNA	SNRTWDCVLV
61	SPRNPQSGFR	LFQLESEADA	LVNFQQYSSQ	LPPFYESSVQ	VLHVEVLQHL	TDLIRNHPS(WO)
121	TVTHLAVELG	IRECFHHSRI	ISCANSTENE	EGCTPLHLAC	RKGDSEILVE	LVQYCHAQMD
181	VTDNKGETAF	HYAVQGDNPQ	VLQLLGKNAS	AGLNQVNNQG	LTPLHLACQ(MO)	GKQEMVRVLL
241	LCNARCNI(MO)G	PGGFPIHTA(MO)	KFSQKGCAE(MO)	IIS(MO)DSNQIH	SKDPRYGASP	LHWAKNAEMA
301	RMLLKRGCDV	DSTSASGNTA	LHVAVTRNRF	D(CO)V(MO)VLLTYG	ANAGARGEHG	NTPLHLA(MO)SK
361	DNMEMVKALI	VFGAEVDTPN	DFGETPAFIA	SKISKQLQDL	(MO)PVSRARKPA	FILSS(MO)RDEK
421	RSHDHLLCLD	GGGVKGLVII	QLLIAIEKAS	GVATKDLFD(WO)	VAGTSTGGIL	ALAILHSKSM
481	AYMRGVYFRM	KDEVFRGSRP	YESGPLEEFL	KREFGEHTKM	TDVKKPKVML	TGTLSDRQPA
541	ELHLFRNYDA	PEAVREPR(CO3)T	PNINLKPPTQ	PADQLVWRAA	RSSGAAPTYF	RPNGRFLDGG
601	LLANNPTLDA	(MO)TEIHEYNQD	(MO)IRKGQGNKV	KKLSIVVSLG	TGKSPQVPVT	(CO)VDVFRPSNP
661	(WO)ELAKTVFGA	KELGKMVVDC	CTDPDGRAVD	RARAWCEMVG	IQYFRLNPQL	GSDIMLDEVS
721	DAVLVNALWE	TEVYIYEHRE	EFQKLVQLLL	SP		

FIGURE 2: Sequence coverage obtained in LC−MS/MS analyses of tryptic digests of oxidant-treated iPLA$_2\beta$ and identified sites of oxidative modification. Only the underlined regions of sequence were not identified in LC−MS/MS analyses of tryptic digests of HOCl-treated iPLA$_2\beta$. MO and WO denote methionine and tryptophan oxidation, respectively. CO denotes sulfenic acid, and CO_3 denotes sulfonic acid.

dependent loss of activity with ~50% inhibition achieved at a concentration of 100 μM (Figure 1B). There was also a corresponding concentration-dependent loss of free thiol groups, but in contrast to the case for H_2O_2-treated iPLA$_2\beta$, activity was incompletely restored (to 71% of the pretreatment level) by incubation with DTT after treatment with the NO donor. This indicates that NO caused some reversible oxidation or nitrosation event(s), perhaps including formation of sulfenic acids and disulfide bonds via Cys-S-NO intermediates (*52*), and also some events that were less readily reversible or irreversible, such as formation of sulfinic or sulfonic acids or other stable adducts (*52*, *55*).

Incubation of iPLA$_2\beta$ with HOCl also resulted in a concentration-dependent loss of activity, with 50 and 90% inhibition achieved at ~30 and ~100 μM HOCl, respectively (Figure 1C), which are concentrations within the ranges observed to affect intracellular processes in intact cells without cell lysis (*62*, *63*, *65*, *69*). This was again associated with a corresponding loss of free thiols, and incubating HOCl-treated iPLA$_2\beta$ with DTT partially restored catalytic activity. Approximately one-third of the lost activity was not restored by DTT, and this presumably reflects formation of stable adducts that cannot be reduced by DTT, such as sulfinic or sulfonic acids, sulfenamides, oxidation products of methionine or tryptophan, or others (*63*, *66*, *83*, *90*−*92*).

Identification of Stable Covalent Modifications of iPLA$_2\beta$ Caused by Biological Oxidants with LC−MS/MS Analyses. Tryptic digests of native and oxidant-treated iPLA$_2\beta$ were analyzed by LC−MS/MS to identify covalent modifications. Through a combination of search algorithms and direct data inspection, more than 73% sequence coverage was achieved for HOCl-treated iPLA$_2\beta$. Figure 2 displays the complete amino acid sequence of iPLA$_2\beta$, and only the underlined regions of sequence were not included in peptides identified by LC−MS/MS analyses of tryptic digests of the oxidant-treated enzyme. Figure 2 also identifies sites where oxidation products of methionine (MO), tryptophan (WO), or cysteine residues were observed.

Cysteine Oxidation. In the case of cysteine, both sulfenic (CO) and sulfonic (CO_3) acid derivatives were observed. Cysteine residues modified in HOCl-treated iPLA$_2\beta$ included Cys332, Cys559, and Cys651. Cys332 and Cys651 were oxidized to sulfenic acids, and the peptides that contained them exhibited an increase in mass of 16 Da compared to the mass of the tryptic peptides expected from the native iPLA$_2\beta$ sequence without modified amino acids, consistent with incorporation of one additional oxygen atom. Cys559 was oxidized to a sulfonic acid, and the peptide that contained it exhibited an increase in mass of 48 Da compared to the mass of the expected native tryptic peptide, consistent with incorporation of three additional oxygen atoms.

Figure 3 is the singly charged MS/MS spectrum produced by deconvolution of the spectrum obtained from CAD of the $[M + 3H]^{3+}$ ion (*m*/*z* 834.39) of the tryptic peptide ^{644}SPQVPVT(CO)VDVFRPSNP(WO)ELAK^{665}. The mass of the parent peptide is thus 2500.17, and the mass expected for the corresponding tryptic peptide from the native iPLA$_2\beta$ sequence is 2468.17. The difference between the observed and expected masses is thus 32, reflecting incorporation of two additional oxygen atoms. Singly charged fragment ions y^{14} (*m*/*z* 1674.01) and y^{15} (*m*/*z* 1792.87) identify Cys651 as the site of incorporation of one oxygen atom because the 119 unit difference between those ions exceeds the Cys residue mass by 16 units.

Tryptophan Oxidation. The observed *m*/*z* value of 1674.01 for the y^{14} fragment ion in Figure 3 is 16 units greater than the expected *m*/*z* value of 1657.9 for the y^{14} ion of the tryptic peptide from the native iPLA$_2\beta$ sequence, suggesting that

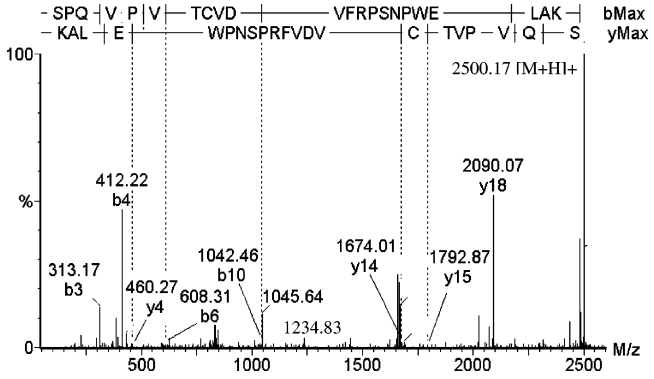

FIGURE 3: Deconvoluted tandem mass spectrum expressed as singly charged ions obtained from collisionally activated dissociation (CAD) of the $[M + 3H]^{3+}$ ion of the oxidized peptide ^{644}SPQVPVT-(CO)VDVFRPSNP(WO)ELAK^{665} in a tryptic digest of oxidant-treated iPLA$_2\beta$. An aliquot (10 μg) of freshly prepared, recombinant, purified iPLA$_2\beta$ was incubated at 37 °C for 30 min with HOCl at a molar ratio of 1:50. The reaction was quenched with a 10-fold molar excess of L-methionine, and digestion with trypsin was performed. The digest was analyzed by LC−MS/MS, and the displayed spectrum of singly charged ions was obtained by CAD of the $[M + 3H]^{3+}$ precursor ion at *m*/*z* 834.39 and deconvolution of the charge states.

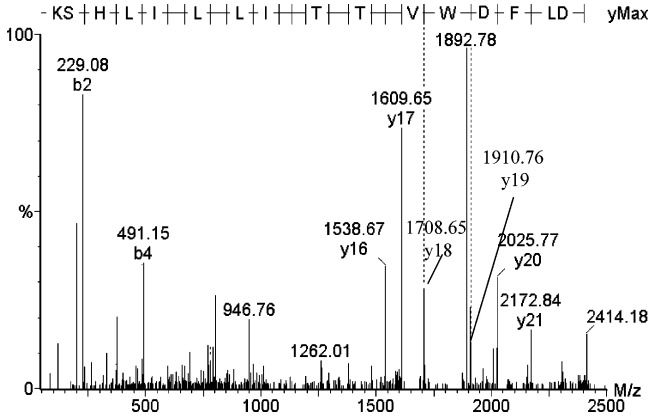

FIGURE 4: Deconvoluted tandem mass spectrum obtained from CAD of the $[M + 3H]^{3+}$ ion (*m*/*z* 801.09) of the oxidized peptide ^{455}DLFD(WO)VAGTSTGGILALAILHSK^{477} in a tryptic digest of oxidant-treated iPLA$_2\beta$.

an amino acid within the native sequence ^{652}VDVFRPSN-PWELAK^{665} of iPLA$_2\beta$ had also been oxidized. The observed *m*/*z* value of 460.27 for the y^4 fragment ion corresponds to that expected for the tryptic peptide from the native iPLA$_2\beta$ sequence, and this indicates that the modified amino acid is contained in the sequence ^{652}VDVFRPSNPW^{661}. An internal fragment ion at *m*/*z* 1234.83 represents the sequence (y^{16})VT(CO)VDVFRPSN(y^6), which indicates that the other oxidized amino acid in the ^{644}S−K^{665} parent peptide is contained within the ^{660}PW^{661} sequence. Because the cyclic proline side chain is much less susceptible to chemical oxidation than the tryptophan aromatic indole ring and because HOCl is known to cause tryptophan oxidation (*91*), W^{661} is the likely site of oxidation.

Tryptophan residues W^{460} and W^{120} were also oxidized in HOCl-treated iPLA$_2\beta$. The former lies near the serine lipase consensus sequence ^{463}GTSTG^{467}, and its oxidation thus might affect catalytic activity. Figure 4 is the tandem spectrum of the tryptic peptide ^{456}DLFD(WO)VAGTSTG-GILALAILHSK^{477} that contains the oxidized W^{460} residue. The 202 unit difference in *m*/*z* values between fragments

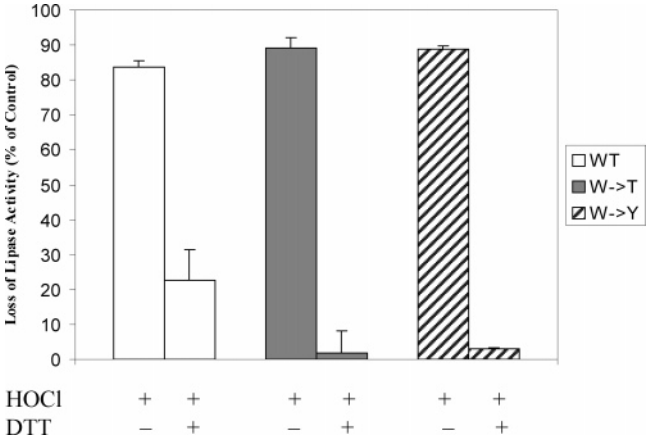

FIGURE 5: Effect of site-directed mutagenesis of iPLA$_2\beta$ residue W^{460} to T or Y on the catalytic activity and susceptibility to irreversible biological oxidant-induced inactivation. The His-tagged mutant proteins iPLA$_2\beta$T^{460} and iPLA$_2\beta$Y^{460} were produced by site-directed mutagenesis, expressed in a baculovirus−Sf9 cell system, and purified by IMAC. Catalytic activities of native iPLA$_2\beta$ and the mutant proteins were then determined before and after treatment with HOCl and then with DTT, as described in the legend of Figure 1. Displayed values represent the loss of activity in the treated samples compared to the control activity of untreated samples and are expressed as means ± SD ($n = 6$).

y^{18} (*m*/*z* 1708.65) and y^{19} (*m*/*z* 1910.76) is 16 units greater than the residue mass of W (186 Da). The strong fragment ion at *m*/*z* 1892.78 is generated from y^{19} (*m*/*z* 1910) by loss of H_2O. Because of the proximity of W^{460} to the iPLA$_2\beta$ active site, its oxidation could play a role in that component of iPLA$_2\beta$ inactivation by HOCl that cannot be reversed by DTT, and this possibility is examined further below with site-directed mutagenesis studies.

Methionine Oxidation. Of the 26 methionine residues in the iPLA$_2\beta$ sequence, 11 were oxidized by HOCl (Figure 2). Only one methionine residue (M^{401}) was oxidized by H_2O_2, and no other amino acid residues were found to incorporate oxygen in H_2O_2-treated iPLA$_2\beta$. This is consistent with the facts that HOCl reacts readily and rather indiscriminately with thiols and thioethers (*63*, *91*) while H_2O_2 tends to selectively modify residues in a protein environment that causes them to be especially reactive (*52*, *55*, *63*). No stable amino acid adducts that had incorporated oxygen were identified in NO-treated iPLA$_2\beta$.

DTT Completely Restores Catalytic Activity to HOCl-Treated iPLA$_2\beta$ Mutant Proteins in Which W^{460} Is Replaced with T^{460} or Y^{460} but Not to HOCl-Treated Native iPLA$_2\beta$. To evaluate the possibility that W^{460} oxidation might play a role in iPLA$_2\beta$ inactivation by HOCl, that residue was replaced with T^{460} or Y^{460} by site-directed mutagenesis. His-tagged native iPLA$_2\beta$ and the mutant proteins iPLA$_2\beta$T^{460} and iPLA$_2\beta$Y^{460} were expressed in a baculovirus−Sf9 cell system and purified by IMAC, and their catalytic activities were then compared before and after HOCl treatment. Both iPLA$_2\beta$ mutant proteins retained essentially full catalytic activity and were nearly completely inactivated by 200 μM HOCl, as was wild-type iPLA$_2\beta$ (Figure 5). Subsequent incubation of the HOCl-treated proteins with DTT restored 97 and 95% of the lost activity of the iPLA$_2\beta$T^{460} and iPLA$_2\beta$Y^{460} mutant proteins, respectively, but DTT restored only 72% of the lost activity of native iPLA$_2\beta$. Mutagenesis of W^{460} to either T or Y thus had little effect per se on

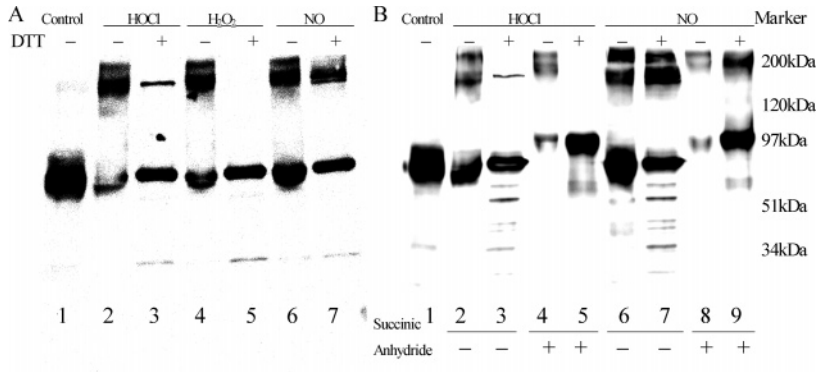

FIGURE 6: Immunoblotting analyses of iPLA$_2\beta$ preparations treated with biological oxidants, dithiothreitol, and succinic anhydride. Aliquots (2 μg) of freshly prepared, purified, recombinant, His-tagged iPLA$_2\beta$ (panels A and B, lane 1) were treated with 200 μM HOCl (panel A, lanes 2−4, and panel B, lanes 2−6), H_2O_2 (panel A, lanes 4−6), or the NO donor diethylamine NONQate (panel A, lanes 6 and 7, and panel B, lanes 6−9). The indicated samples (panel A, lanes 3, 5, and 7, and panel B, lanes 3, 5, 7, and 9) were then incubated with 2.5 mM DTT at 37 °C for 30 min. In panel B (lanes 4, 5, 8, and 9), the indicated samples were treated with 4.5 μg/μL succinic anhydride. SDS−PAGE analyses were then performed under nonreducing conditions, and immunoblotting was performed with iPLA$_2\beta$ antibodies after the transfer to PVDF membranes.

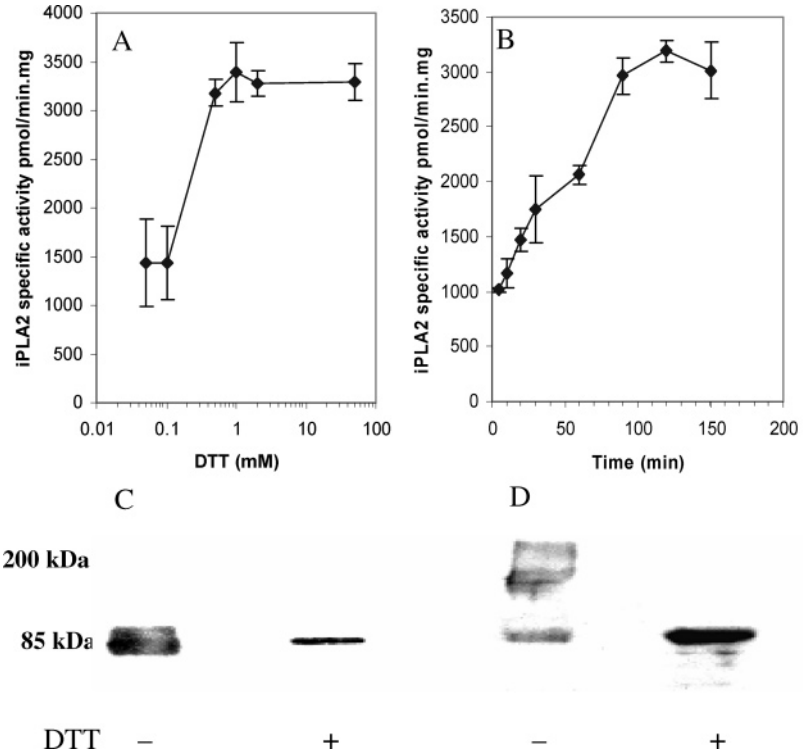

FIGURE 7: Effects of dithiothreitol on time-dependent changes in the iPLA$_2\beta$ catalytic activity and oligomerization state that occur during storage. Samples (50 pmol) of recombinant, purified, His-tagged iPLA$_2\beta$ that had been stored at 4 °C for 2 weeks were incubated with 2 mM DTT at room temperature for various (0−150 min) intervals (A) or with varied concentrations (0−50 mM) of DTT for 60 min (B), and iPLA$_2\beta$ activity was then measured. Displayed values represent means ± SD ($n = 6$). Aliquots (2 μg) of iPLA$_2\beta$ that had been freshly prepared (C) or stored at 4 °C for 2 weeks (D) were also analyzed by nonreducing SDS−PAGE and immunoblotting before (left-most lanes of panels C and D) or after (right-most lanes of panels C and D) incubation with 2.5 mM DTT at 37 °C for 30 min. Immunoblots were probed with antibodies to iPLA$_2\beta$.

iPLA$_2\beta$ activity but nearly eliminated the component of iPLA$_2\beta$ inactivation by HOCl that cannot be reversed by DTT. W^{460} oxidation thus could be involved in irreversible iPLA$_2\beta$ inactivation.

Evidence for Formation of Intermolecular Disulfide Bonds upon Treatment of iPLA$_2\beta$ with Biological Oxidants. Immunoblotting analyses indicate that treating iPLA$_2\beta$ with H_2O_2, NO, or HOCl causes the enzyme to form higher-molecular mass species that could reflect formation of intermolecular disulfide bonds (Figure 6). Treatment with HOCl resulted in the most dramatic reduction in intensity of the monomeric 85 kDa iPLA$_2\beta$-immunoreactive band (Figure 6A, lane 2), and HOCl also caused a greater reduction in iPLA$_2\beta$ thiol content at a given oxidant concentration than did H_2O_2 or NO (Figure 1). All oxidant-treated samples exhibited a broad region of poorly resolved higher-molecular mass iPLA$_2\beta$-immunoreactive species on SDS−PAGE (Figure 6).

For H_2O_2-treated iPLA$_2\beta$ samples, incubation with DTT before SDS−PAGE analysis caused the disappearance of the higher-molecular mass species, and only a single 85 kDa iPLA$_2\beta$-immunoreactive band was observed (Figure 6A, lane 5). This is consistent with the fact that incubation with DTT completely restored the free thiol content and activity of

H_2O_2-treated iPLA$_2\beta$ (Figure 1) and suggests that H_2O_2 induces intermolecular disulfide bond formation between iPLA$_2\beta$ monomers.

Biological Oxidant-Induced iPLA$_2\beta$ Oligomerization by Mechanisms Other Than Intermolecular Disulfide Bond Formation. In contrast, incubating HOCl-treated iPLA$_2\beta$ with DTT did not cause the complete disappearance of the higher-molecular mass immunoreactive species, but their intensity was reduced while that of the 85 kDa monomer increased (Figure 6A, lane 3). In addition, a single, sharp higher-molecular mass band of ~200 kDa was observed after HOCl-treated iPLA$_2\beta$ was incubated with DTT rather than the broad region of poorly resolved bands observed before incubation with DTT. Similarly, incubating NO-treated iPLA$_2\beta$ with DTT caused a reduction in both the intensity and the heterogeneity of the higher-molecular mass iPLA$_2\beta$-immunoreactive bands and the appearance of a sharply focused 85 kDa band (Figure 6A, lane 7).

The DTT-resistant higher-molecular mass iPLA$_2\beta$-immunoreactive bands produced by treatment with HOCl or with NO might represent oligomers stabilized by strong, noncovalent interactions. Treating apomyoglobin with HOCl causes the appearance of such oligomers, and they can be disrupted by charge repulsion when positively charged amino acids are converted to anions by treatment with succinic anhydride (93). Upon incubation of HOCl-treated iPLA$_2\beta$ with succinic anhydride, the DTT-resistant 200 kDa iPLA$_2\beta$-immunoreactive band (Figure 6A,B, lane 3) did disappear (Figure 6B, lane 5), and this band could thus represent an oligomer formed by noncovalent interactions. In contrast, incubating NO-treated iPLA$_2\beta$ with succinic anhydride did not cause the complete disappearance of the DTT-resistant higher-molecular mass iPLA$_2\beta$-immunoreactive bands, but it did reduce their heterogeneity and that of the 85 kDa monomer (Figure 6B, lane 9). NO must, therefore, induce oligomeriztion of iPLA$_2\beta$ by mechanisms in addition to forming intermolecular disulfide bonds and noncovalent complexes.

Time- and Temperature-Dependent Inactivation of iPLA$_2\beta$ and Thiol Oxidation. Upon storage at 4 °C for 2 weeks, the specific activity of recombinant, purified His-tagged iPLA$_2\beta$ fell to ~20% of initial values (not shown). Treating iPLA$_2\beta$ samples at that point with DTT resulted in a concentration- and time-dependent increase in activity (Figure 7A,B), although such an effect was not observed with freshly prepared iPLA$_2\beta$ (not shown). These findings suggest that reversible thiol oxidation contributes to the loss of activity upon storage of iPLA$_2\beta$.

Consistent with that possibility, immunoblotting analyses of iPLA$_2\beta$ that had been freshly prepared (Figure 7C) or stored for 2 weeks at 4 °C (Figure 7D) revealed that storage was associated with the appearance of higher-molecular mass iPLA$_2\beta$-immunoreactive bands that were not observed in fresh iPLA$_2\beta$ preparations. These higher-molecular mass bands disappeared upon incubation with DTT (Figure 7D), suggesting that they represented iPLA$_2\beta$ oligomers formed by intermolecular disfulfide bonds. Because incubation with DTT also increased the activity of stored iPLA$_2\beta$ preparations (Figure 7A,B), these observations suggest that intermolecular disulfide bond formation contributes to the loss of activity.

iPLA$_2\beta$ undergoes thermal inactivation upon incubation at 37 °C that is largely prevented by including ATP in the incubation medium (*94*, *95*). We found that DTT exerts an

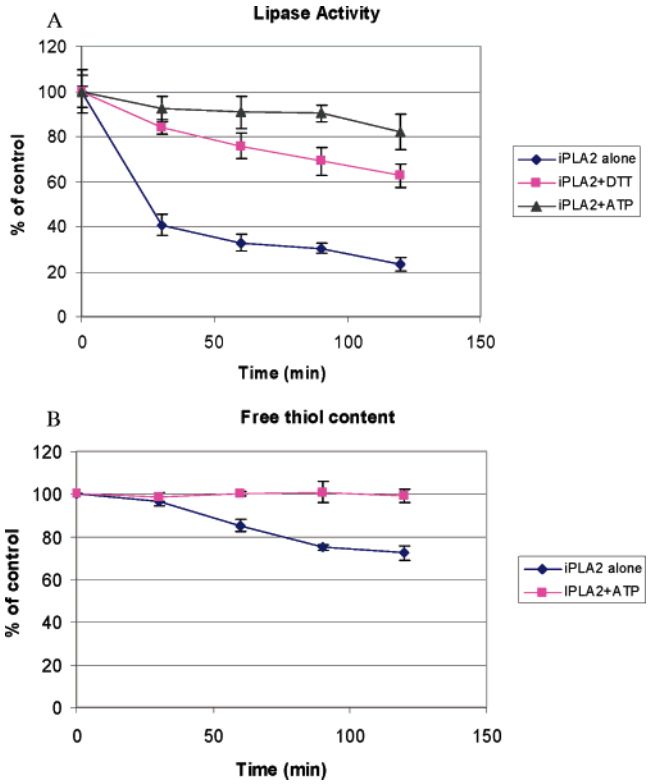

FIGURE 8: Effects of dithiothreitol and ATP on the thermal inactivation and thiol content of iPLA$_2\beta$. Freshly prepared, recombinant, purified, His-tagged iPLA$_2\beta$ was incubated with vehicle only (▲), with 2.5 mM DTT (■), or with 10 mM ATP (◆) at 37 °C for various (0−120 min) intervals, and aliquots were removed for measurement of enzymatic activity (A) and thiol content (B). Displayed values represent means ± SD ($n = 6$).

effect similar to that of ATP to attenuate thermal inactivation of iPLA$_2\beta$ (Figure 8A) and that incubating iPLA$_2\beta$ at 37 °C also results in the loss of free thiols that is prevented by ATP (Figure 8B). Incubating iPLA$_2\beta$ at 37 °C also resulted in the appearance of higher-molecular mass iPLA$_2\beta$-immunoreactive bands on SDS−PAGE that disappeared upon treatment with DTT, and the appearance of these bands was prevented by including ATP in the incubation medium (not shown). This suggests that thermal inactivation of iPLA$_2\beta$ is associated with thiol oxidation that is prevented by ATP. There are ATP binding sites in the iPLA$_2\beta$ sequence (*24*, *96*), and binding might affect the conformation of iPLA$_2\beta$ in a way that protects critical thiol groups from oxidation.

The data in Figure 8 also suggest that thiol oxidation is not the sole mechanism contributing to iPLA$_2\beta$ thermal inactivation and that ATP protects against inactivation by mechanisms in addition to preventing thiol oxidation. Approximately 80% of iPLA$_2\beta$ activity is lost after incubation at 37 °C for 2 h (Figure 8A), but only 30% of the free thiol content is lost. ATP confers complete protection against thiol loss (Figure 8B) but incomplete protection against loss of activity. This could indicate that the loss of certain critical thiols has a larger effect on activity than the loss of others and/or that activity is also lost by mechanisms independent of thiol loss. Approximately 20% of initial activity is lost even in the presence of ATP. Similarly, DTT provides partial but incomplete protection against thermal inactivation (Figure 8A) but presumably complete protection against thiol loss. (The presence of DTT in the incubation medium prevents

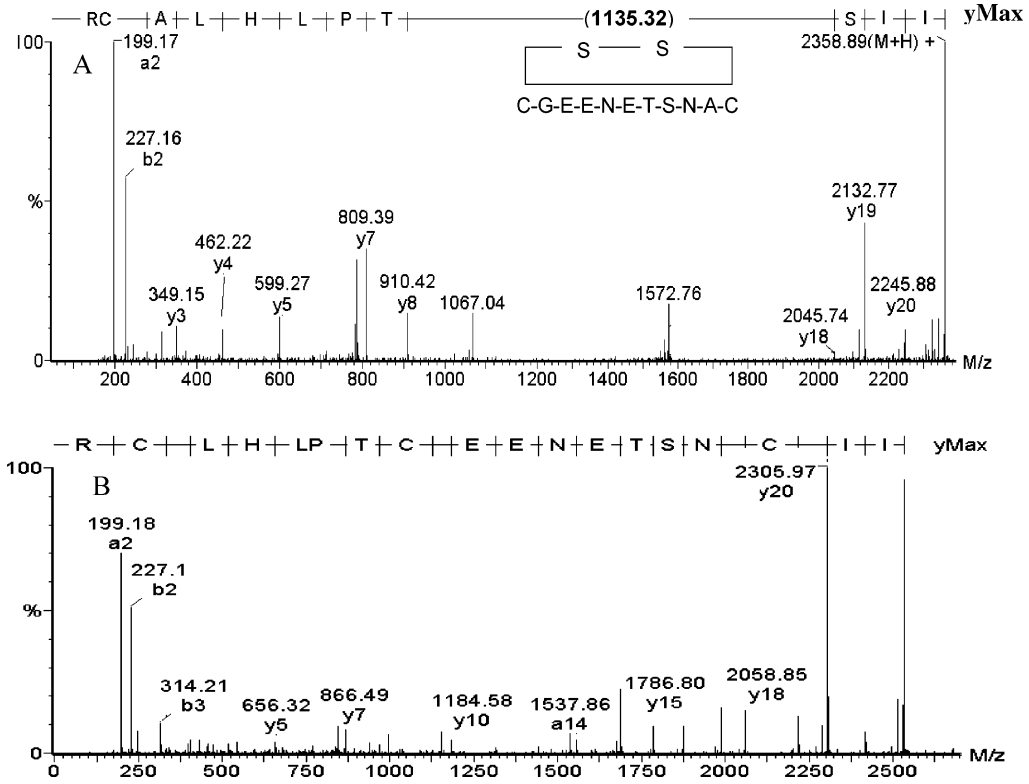

FIGURE 9: Demonstration of an intramolecular disulfide bond between Cys143 and Cys153 in the iPLA$_2\beta$ tryptic peptide ^{140}IISCANSTENEEGCTPLHLACR^{161} by tandem MS. Panel A is the deconvoluted MS/MS spectrum obtained from CAD of the $[M + 3H]^{3+}$ precursor ion at *m*/*z* 786.96 and demonstrates that the parent peptide contains a disulfide bond between Cys143 and Cys153. Panel B is the analogous MS/MS spectrum obtained from CAD of the $[M + 3H]^{3+}$ precursor ion at *m*/*z* 844.68 after reduction and carboxyamidomethylation of the parent peptide.

direct measurement of iPLA$_2\beta$ free thiol content.) Approximately 40% of the initial activity is lost in the presence of DTT. These data thus suggest that, of the activity lost after incubation of iPLA$_2\beta$ at 37 °C for 2 h, ~50% is attributable to thiol oxidation that is prevented by DTT (or ATP) and ~25% occurs by some other mechanism that is prevented by ATP. Another 25% of the activity loss occurs by a mechanism(s) that is unaffected by ATP.

Identification of iPLA$_2\beta$ Disulfide Bonds by LC−MS/MS. Treatment of freshly prepared iPLA$_2\beta$ with DTT resulted in decreased heterogeneity of the 85 kDa iPLA$_2\beta$ monomer band (Figure 7C), suggesting that heterogeneity might arise from varied degrees of intramolecular disulfide bonding within the population of iPLA$_2\beta$ monomers. To examine this possibility, the heterogeneous 85 kDa monomer band of freshly prepared iPLA$_2\beta$ analyzed by SDS−PAGE was excised and digested in gel with trypsin. The digest was then analyzed by LC−MS/MS, and ~700 MS/MS spectra so acquired were analyzed by a modified Signature Discovery program (*84*) that facilitates identification of disulfide-linked peptides.

The internal disulfide-linked peptide ^{140}IIS(C-S-)ANSTENEEG(C-S-)TPLHLACR^{161} was so identified. It contains Cys143, Cys153, and Cys160. The observed *m*/*z* value for the precursor ion of the digest peptide representing ^{140}I−R^{161} is 786.96. Therefore, the calculated molecular mass of the parent peptide is 2358 Da. This is 2 Da less than the theoretical mass of 2360 Da for the tryptic peptide ^{140}I−R^{161} from the native sequence, and this suggests that two of the three Cys residues are linked by a disulfide bond. Figure 9A is the deconvoluted MS/MS spectrum obtained from CAD of the $[M + 3H]^{3+}$ ion at *m*/*z* 786.96. The N-terminal sequence ISS and the C-terminal sequence TPLHLACR are identified by matching theoretical fragment ions with intense peaks in the spectrum. The sequence between Cys143 and Cys153 is not represented by fragment ions because the disulfide bond between these two residues suppresses fragmentation. The difference in *m*/*z* values between the singly charged y^8 and y^{19} ions in the spectrum is 1135.32, which is 2 units less than the theoretical mass of the internal fragment ^{143}CANGTENEEGC^{153} (1137.37 Da). The intense ion at *m*/*z* 1067 corresponds to the internal fragment ^{144}ANGTENEEGC^{153} or ^{143}CANGTENEEG^{152} (theoretical mass of 1035.4 Da) with an additional sulfur (32 Da) atom derived from the disulfide bond. Figure 8B is the MS/MS spectrum of peptide ^{140}IIS(C-S-)ANSTENEEG(C-S-)TPLHLACR^{161} after reduction with DTT and carboxyamidomethylation with iodoacetamide.

Another disulfide-linked peptide was identified from the iPLA$_2\beta$ C-terminal region. The deconvoluted MS/MS spectrum (Figure 10) obtained from CAD of the $[M + 2H]^{2+}$ ion at *m*/*z* 654.76 from the iPLA$_2\beta$ tryptic digest reveals an internal disulfide bond between Cys679 and Cys680. The mass of the identified peptide (^{675}MVVDCCTDPDGR^{686}) (Figure 10A) is 1307 Da, which is 2 Da less than the theoretical value of 1309 Da for tryptic peptide ^{675}M−R^{686} from the native iPLA$_2\beta$ sequence. All of the expected y-series ions are observed in the MS/MS spectrum except for the y^7 ion, which arises from cleavage of the disulfide bond between the two cysteines. The difference in *m*/*z* values between y^6 (*m*/*z* 660.27) and y^8 (*m*/*z* 864.29) is 204 units, which is also 2 units less than the expected difference of 206 units if there

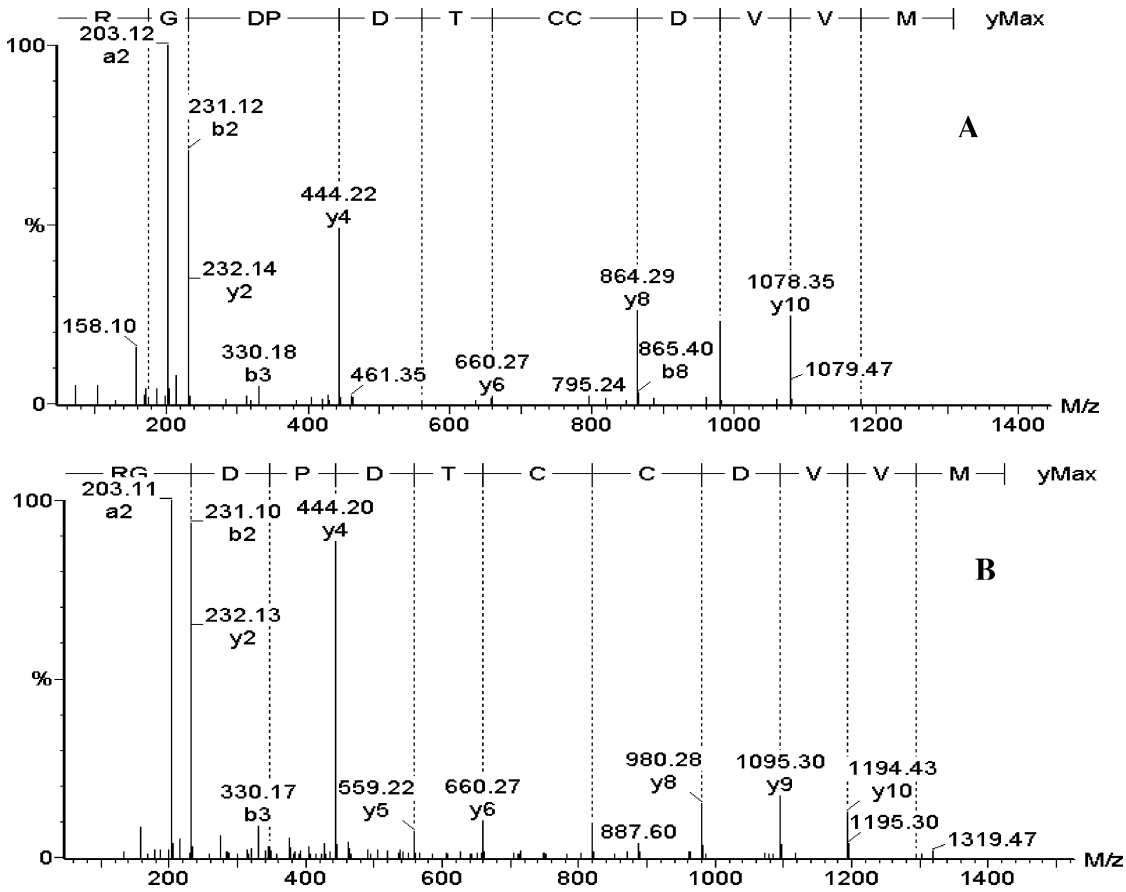

FIGURE 10: Demonstration of an intramolecular disulfide bond between Cys679 and Cys680 in the iPLA$_2\beta$ tryptic peptide ^{675}MVVDCCTDPDGR^{686} by tandem MS. Panel A is the deconvoluted MS/MS spectrum obtained from CAD of the $[M + 2H]^{2+}$ precursor ion at *m*/*z* 654.72 and demonstrates that the parent peptide contains a disulfide bond between Cys679 and Cys680. Panel B is the analogous MS/MS spectrum obtained from CAD of the $[M + 2H]^{2+}$ precursor ion at *m*/*z* 712.73 after reduction and carboxyamidomethylation of the parent peptide.

were no disulfide bonds in the intervening sequence. After reduction and carboxyamidomethylation, the mass of the parent peptide ^{675}MVVDCCTDPDGR^{686} increased to 1424 Da, and its MS/MS spectrum contains a strong y^7 ion at *m*/*z* 820.28 (Figure 10B). The observed mass is consistent with modification of the two Cys residues in this peptide by carboxyamidomethylation, resulting in a 114 Da increase in mass.

Effects of Oxidative Stress in INS-1 Insulinoma Cells on iPLA$_2\beta$ Oligomerization State, Subcellular Distribution, and Activity. Diamide is a cell-permeant, thiol-specific oxidant that induces mild, noninjurious oxidative stress and disulfide bond formation in intact cells (*89*, *97*). INS-1 insulinoma cells that overexpress EGFP-tagged iPLA$_2\beta$ (*87*) were incubated with diamide and then studied by cytofluorescence microscopy or lysed for iPLA$_2\beta$ immunoblotting and activity assays. Treating the cells with diamide induced the appearance of a high-molecular mass iPLA$_2\beta$-immunoreactive band upon SDS−PAGE analyses (Figure 11A). This was associated with accumulation of EGFP-iPLA$_2\beta$ into a punctate pattern within the cells on cytofluorescence analyses (Figure 11B) reminiscent of that induced by treating INS-1 cells with thapsigargin to deplete ER Ca^{2+} stores or with cAMP-elevating agents (*33*, *87*). Incubating the cells with diamide also caused a decline in iPLA$_2\beta$ activity (Figure 11C) and a concentration-dependent decrease in the rate of release of [^{3}H]arachidonic acid into the incubation medium (Figure 11D) from cells whose phospholipids had been prelabeled with [^{3}H]arachidonic acid.

DISCUSSION

The recent demonstration that the widely used iPLA$_2\beta$ inhibitor BEL inactivates the enzyme by alkylating critical Cys thiols (*50*) raises the possibility that thiol modification by biological redox reactions might affect the activity or other properties of the enzyme. Such reactions play important regulatory roles in a variety of biological phenomena (*51*−*54*). Because many cells that express iPLA$_2\beta$ produce biological oxidants that can modify thiols, it is likely that the enzyme is exposed to such molecules in vivo. iPLA$_2\beta$ is expressed in phagocytes, for example, and is a required participant in transcriptional events involved in increasing phagocyte expression of inducible NO synthase (iNOS) in response to viral infection (*37*). Phagocytes thus can produce NO via iNOS, and they also produce O^{2-} via NADPH oxidase, which dismutates to H_2O_2 that is used by the phagocyte enzyme MPO to generate HOCl (*60*−*63*).

Phagocyte-derived HOCl is also thought to affect proliferation and other properties of vascular wall cells (*68*, *77*), and iPLA$_2\beta$ is expressed in such cells and participates in regulating their proliferation (*43*, *80*). Similarly, iPLA$_2\beta$ is expressed in insulin-secreting β-cells (*13*), which produce both NO via iNOS (*78*, *79*) and O^{2-}/H_2O_2 through mitochondrial metabolism and other pathways (*73*−*77*). We have also found that β-cells express MPO (S. Bao and J. Turk,

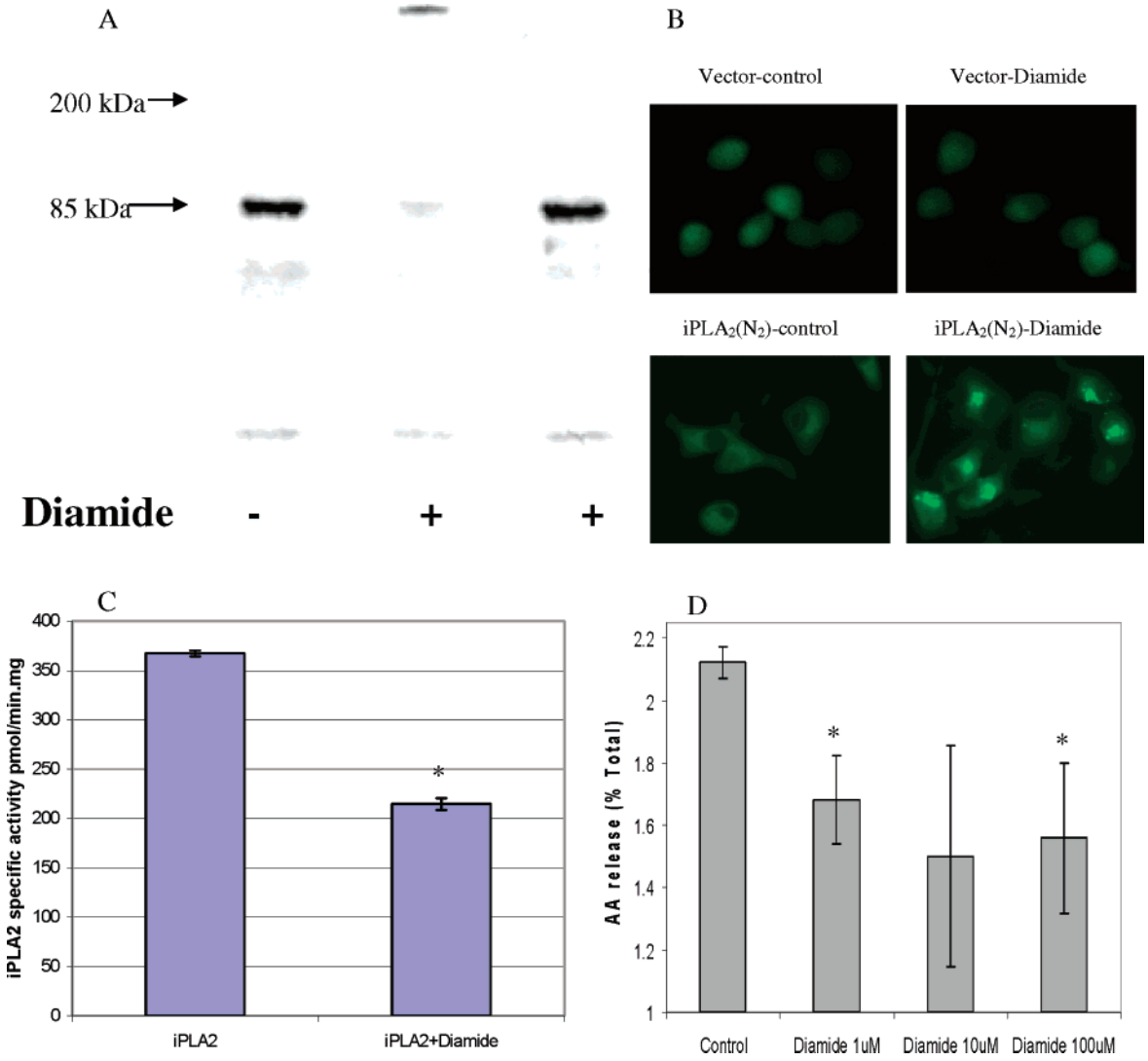

FIGURE 11: Effects of oxidative stress caused by treating INS-1 insulinoma cells with the cell-permeant thiol oxidant diamide on iPLA$_2\beta$ oligomerization state, subcellular distribution, and catalytic activity. INS-1 insulinoma cells that express EGFP-tagged iPLA$_2\beta$ were incubated (37 °C for 10 min) with diamide (5 mM). Aliquots of cell suspensions were removed before (A, lane 1) and after (A, lanes 2 and 3) incubation with diamide and then treated (A, lane 3) or not treated (A, lanes 1 and 2) with 2.5 mM DTT and analyzed by SDS−PAGE under nonreducing conditions. Immunoblotting was then performed with iPLA$_2\beta$ antibody after transfer to PVDF membranes (A). In panel B, fluorescence microscopic analyses were performed with INS-1 cells infected with an empty viral vector (top micrographs) or with a viral vector containing cDNA encoding EGFP-tagged iPLA$_2\beta$ (bottom micrographs) and incubated without (left micrographs) or with (right micrographs) diamide (5 mM). In panel C, iPLA$_2\beta$ catalytic activity was determined in aliquots of lysates from INS-1 cells that had been incubated without (left bar) or with (right bar) diamide (5 mM). In panel D, INS-1 cells were preincubated with [^{3}H]arachidonic acid to label their phospholipids and then washed to remove unincorporated radiolabel. Aliquots of cell suspensions were then seeded onto 16-well plates and incubated (30 min at 37 °C under 95% air and 5% CO_2) with the indicated concentrations of diamide. Aliquots of media were then removed for determination of the amount of released [^{3}H]arachidonic acid by liquid scintillation spectrometry. Displayed values represent means ± SD ($n = 6$). Asterisks indicate $p < 0.05$ vs the control condition.

unpublished observations), as do neurons (*70*), and iPLA$_2\beta$ is the major PLA$_2$ in brain neurons (*81*, *82*). It is thus likely that iPLA$_2\beta$ is exposed to H_2O_2, NO, and HOCl in various cellular contexts, and these biological oxidants could affect the function of the enzyme. Characterizing such effects could be important because factors that regulate iPLA$_2\beta$ activity and subcellular distribution are much less well understood than those that affect the better-studied enzyme cPLA$_2\alpha$ (*3*, *6*).

Our observations indicate that biological concentrations of H_2O_2 inactivate iPLA$_2\beta$, and this can be completely reversed by subsequent incubation with DTT. This suggests that inactivation results from covalent modifications that can be reduced by DTT, such as formation of disulfide bonds or sulfenic acids (*52*, *55*). Inactivation of iPLA$_2\beta$ by NO or HOCl also can be partially reversed by DTT, and this presumably reflects similar covalent modifications of the enzyme. NO- or HOCl-induced iPLA$_2\beta$ inactivation also has a component that cannot be reversed by DTT, and this presumably reflects DTT-resistant covalent modifications, such as formation of sulfonic acids, Trp oxides, Met sulfoxides, or others (*52*, *55*).

DTT-reversible covalent modifications were observed upon LC−MS/MS analyses of tryptic digests of oxidant-treated iPLA$_2\beta$. Cys332 and Cys651, for example, were converted to sulfenic acid derivatives upon oxidant treatment, and Cys559 was further oxidized to the stable sulfonic acid derivative. In previous studies, Cys was the only amino acid

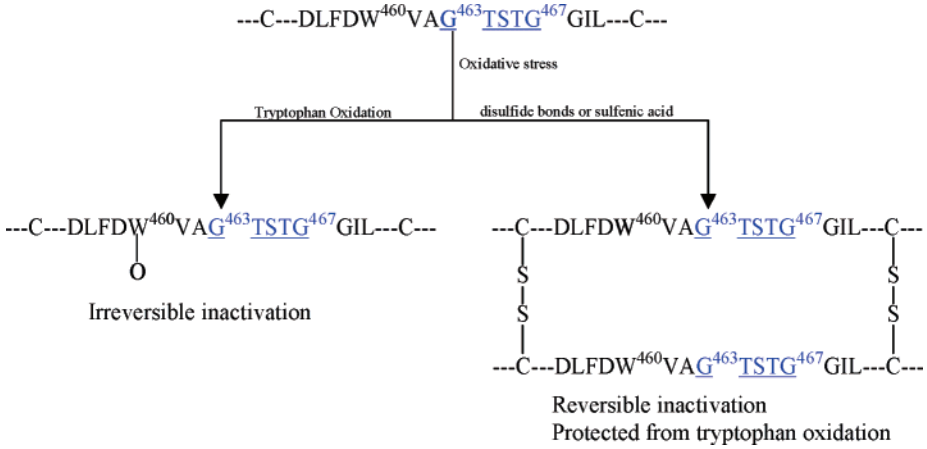

FIGURE 12: Reversible and irreversible oxidative covalent modifications of iPLA$_2\beta$ and modes of catalytic inactivation. Treatment of iPLA$_2\beta$ with biological oxidants reduces catalytic activity, and this is partially but incompletely reversed by dithiothreitol, indicating that there are reversible and irreversible modes of oxidative inactivation. Some covalent modifications induced by oxidants, e.g., formation of Cys-sulfenic acids or disulfide bonds, can also be reversed upon incubation with DTT, while others, e.g., Trp oxidation or formation of Met sulfoxide or Cys sulfonic acids, are not reversible.

residue observed to be modified during the inactivation of iPLA$_2\beta$ and its covalent modification by the suicide substrate BEL, and modification of Cys651 correlated most closely with BEL-induced inactivation of iPLA$_2\beta$ (*50*). Moreover, site-directed mutagenesis of Cys651 to Ala yielded an active mutant enzyme with reduced sensitivity to inhibition (*50*). It is thus possible that oxidation of Cys651 to a sulfenic acid might be a mechanism for regulating iPLA$_2\beta$ activity that would be reversible by subsequent reduction to the free thiol.

Formation of cysteine sulfenic acid (Cys-SOH) residues in iPLA$_2\beta$ upon treatment with biological oxidants is of interest because protein-sulfenic acids are now recognized to play important roles in redox regulation (*51*−*55*, *98*). Cys-SOH formation causes reversible inhibition of protein tyrosine phosphatases (*99*, *100*) and glutathione reductase (*101*) during tyrosine phosphorylation-dependent signal transduction events and nitrosative stress, respectively. Cys-SOH also participates in the redox regulation of transcription factors such as Fos, c-Jun/Activator protein-1 and bovine papillomavirus-1 E2 protein (*102*−*104*).

A second class of DTT-reversible covalent modifications of oxidant-treated iPLA$_2\beta$ that was identified is disulfide bond formation. Intramolecular disulfide bonds (Cys143-S-S-Cys153 and Cys679-S-S-Cys680) were also identified in fresh iPLA$_2\beta$ preparations even under conditions where free thiol groups were blocked, suggesting that these bonds were not generated during processing and may exist in the enzyme within cells. Incubating freshly prepared iPLA$_2\beta$ with DTT reduced these bonds but caused little change ($\leq$20% increase) in activity, suggesting that the bonds may not be critical in regulating catalytic activity, although they could have a role in governing the interaction of the enzyme with other proteins (*86*) or its subcellular distribution (*87*).

Intermolecular disulfide bond formation appears to be involved in the spontaneous time- and temperature-dependent oxidation of iPLA$_2\beta$ that occurs without exposure to added biological oxidants, and this is also associated with the loss of enzymatic activity. That intermolecular disulfide bond formation could affect properties of iPLA$_2\beta$ in vivo is suggested by the facts that subjecting INS-1 insulinoma cells to mild oxidative stress with diamide induced formation of iPLA$_2\beta$-immunoreactive oligomers that could be reduced by DTT and that this was associated with the loss of iPLA$_2\beta$ activity in cell lysates, the subcellular redistribution of EGFP-tagged iPLA$_2\beta$ on cytofluorescence analyses, and a reduction in the rate of release of [^{3}H]arachidonic acid from membrane phospholipids.

Although spontaneous, time- and temperature-dependent oxidative inactivation of iPLA$_2\beta$ has a component that can be reversed by incubation with DTT, there is another component that is not. Binding of ATP appears to reduce both modes of inactivation, possibly by causing the enzyme to adopt a conformation that renders it less susceptible to oxidation. Such a conformational change might be involved in the effect of ATP to prevent completely the time- and temperature-dependent loss of free thiol groups in iPLA$_2\beta$, and protection against thiol oxidation might account for the long recognized but previously unexplained effect of ATP in attenuating iPLA$_2\beta$ thermal inactivation (*94*, *95*). There is also a component of time- and temperature-dependent iPLA$_2\beta$ inactivation that is not prevented by ATP or reversed by DTT.

Covalent modifications that cannot be reversed by DTT that were observed upon LC−MS/MS analyses of tryptic digests of oxidant-treated iPLA$_2\beta$ included formation of sulfonic acids, Trp oxides, and Met sulfoxides. Although Trp and Met oxidation can occur during sample processing, such oxidations can also serve regulatory functions in vivo. Oxidation of a specific Trp residue (W^{60}) in B-crystallin has been demonstrated (*105*), and oxidation of a critical conserved Trp residue (W^{352}) in luminal loop E of chloroplast photosystem II protein CP43 is a highly selective in vivo modification (*106*). Oxidation of a methionine residue (M^{110}) to the sulfoxide in cathepsin G targets the enzyme for proteolysis (*107*). The oxidized residue W^{460} identified here in oxidant-treated iPLA$_2\beta$ is located near the serine lipase consensus sequence (^{463}GTSTG^{467}), and its oxidation could represent one mechanism for irreversible iPLA$_2\beta$ inactivation. That possibility is consistent with our finding that mutagenesis of W^{460} to less readily oxidizable residues yields active mutant enzymes that no longer exhibit a DTT-irreversible component of HOCl-induced inactivation.

In summary, two distinct modes of iPLA$_2\beta$ inactivation occur upon exposure to biological oxidants (Figure 12). One

can be reversed by DTT and is associated with formation of higher-molecular mass oligomers that can be reduced by DTT. DTT-reversible oxidation events could include formation of Cys-sulfenic acid derivatives and/or of Cys-Cys disulfide bonds, and both were observed in oxidant-treated iPLA$_2\beta$. Formation of Cys651-sulfenic acid could represent one mechanism for DTT-reversible iPLA$_2\beta$ inactivation because alkylation of that residue by the suicide substrate BEL is strongly associated with loss of activity, and mutagenesis to a nonalkylatable residue reduces the sensitivity to inhibition (*50*). Another mode of oxidative iPLA$_2\beta$ inactivation cannot be reversed with DTT and could be caused by Trp or Met oxidation or by formation of Cys-sulfonic acid derivatives, and all of these modifications were also observed in oxidant-treated iPLA$_2\beta$. W^{460} oxidation could represent one mechanism for irreversible iPLA$_2\beta$ inactivation because of the proximity of that residue to the ^{463}GTSTG^{467} catalytic center and because its mutagenesis to a less readily oxidizable residue protects against irreversible inactivation. Although the relevance of these studies to biological function within cells remains unproven as yet, the findings described above and the observation that subjecting insulinoma cells to mild oxidative stress affects iPLA$_2\beta$ oligomerization state, activity, and subcellular distribution and alters release of arachidonic acid from phospholipids suggest that iPLA$_2\beta$ might be subject to intracellular redox regulation.

ACKNOWLEDGMENT

We thank Dr. Mary Wohltmann, Alan Bohrer, Wu Jin, and Sheng Zhang for excellent technical assistance and Jessica Jackson for secretarial assistance.

REFERENCES

1. Brash, A. R. (2001) Arachidonic acid as a bioactive molecule, *J. Clin. Invest. 107*, 1339−45.
2. Radu, C. G., Yang, L. V., Riedinger, M., Au, M., and Witte, O. N. (2004) T cell chemotaxis to lysophosphatidylcholine through the G2A receptor, *Proc. Natl. Acad. Sci. U.S.A. 101*, 245−50.
3. Six, D., and Dennis, E. (2000) The expanding superfamily of phospholipase A$_2$ enzymes: Classification and characterization, *Biochim. Biophys. Acta 1488*, 1−19.
4. Ma, Z., and Turk, J. (2001) The molecular biology of the Group VIA Ca^{2+}-independent phospholipase A$_2$, *Prog. Nucleic Acid Res. Mol. Biol. 67*, 1−33.
5. Murphy, R. C., and Fitzpatrick, F. A. (1990) Arachidonate related lipid mediators, *Methods Enzymol. 187*, 1−628.
6. Gijon, M., Spencer, D., Kaiser, A., and Leslie, C. (1999) Role of phosphorylation sites and the C2 domain in regulation of cytosolic phospholipase A$_2$, *J. Cell Biol. 145*, 1219−32.
7. Underwood, K. W., Song, C., Kriz, R. W., Chang, X. J., Knopf, J. L., and Lin, L. L. (2002) A novel calcium-independent phospholipase A$_2$, cPLA$_2\gamma$, that is prenylated and contains homology to cPLA$_2$, *J. Biol. Chem. 273*, 21926−32.
8. Pinckard, R. T., Strifle, B. A., Kramer, R. M., and Sharp, J. D. (1999) Molecular cloning of two new human paralogs of 85 kDa cytosolic phospholipase A$_2$, *J. Biol. Chem. 274*, 8823−31.
9. Song, C., Chang, X. J., Bean, K. M., Proia, M. S., Knopf, J. L., and Kriz, R. W. (1999) Molecular characterization of cytosolic phospholipase A$_2\beta$, *J. Biol. Chem. 274*, 17063−7.
10. Ohto, T., Uozumi, N., Hirabayashi, T., and Shimuzu, T. (2005) Identification of novel cytosolic phospholipase A$_2$s, murine cPLA$_2\delta$, ϵ, and ζ, which form a gene cluster with cPLA$_2\beta$, *J. Biol. Chem. 280*, 24576−83.
11. Tang, J., Kriz, R. W., Wolfman, N., Shaffer, M., Seehra, J., and Jones, S. S. (1997) A novel cytosolic calcium-independent phospholipase A$_2$ contains eight ankyrin motifs, *J. Biol. Chem. 272*, 8567−75.
12. Balboa, M. A., Balsinde, J., Jones, S., and Dennis, E. A. (1997) Identity between the calcium-independent phospholipase A$_2$ enzymes from P388D1 macrophages and Chinese hamster ovary cells, *J. Biol. Chem. 272*, 8576−90.
13. Ma, Z., Ramanadham, S., Kempe, K., Chi, X. S., Ladenson, J., and Turk, J. (1997) Pancreatic islets express a Ca^{2+}-independent phospholipase A$_2$ enzyme that contains a repeated structural motif homologous to the integral membrane protein binding domain of ankyrin, *J. Biol. Chem. 272*, 11118−27.
14. Balsinde, J., and Dennis, E. A. (1997) Function and inhibition of intracellular calcium-independent phospholipase A$_2$, *J. Biol. Chem. 272*, 16069−72.
15. Hazen, S. L., Zupan, L. A., Weiss, R. H., Getman, D. P., and Gross, R. W. (1991) Suicide inhibition of canine myocardial cytosolic calcium-independent phospholipase A$_2$. Mechanism-based discrimination between calcium-dependent and -independent phospholipases A$_2$, *J. Biol. Chem. 266*, 7227−32.
16. Zupan, L. A., Weiss, R. H., Hazen, S., Parnas, B. L., Aston, K. W., Lennon, P. J., Getman, D. P., and Gross, R. W. (1993) Structural determinants of haloenol lactone-mediated suicide inhibition of canine myocardial calcium-independent phospholipase A$_2$, *J. Med. Chem. 36*, 95−100.
17. Ma, Z., Ramanadham, S., Hu, Z., and Turk, J. (1998) Cloning and expression of a type IV cytosolic phospholipase A$_2$ enzyme from a pancreatic islet cDNA library. Comparison of the expressed activity with that of the islet type VI cytosolic phospholipase A$_2$, *Biochim. Biophys. Acta 1391*, 384−400.
18. Balsinde, J., and Dennis, E. A. (1996) Distinct roles in signal transduction for each of the phospholipase A$_2$ enzymes present in P388D1 macrophages, *J. Biol. Chem. 271*, 6758−65.
19. Mancuso, D., Jenkins, C. M., and Gross, R. W. (2000) The genomic organization, complete mRNA sequence, cloning, and expression of a novel human intracellular membrane-associated calcium-independent phospholipase A$_2$, *J. Biol. Chem. 275*, 9937−45.
20. Tanaka, H., Takeya, R., and Sumimoto, H. (2000) A novel intracellular membrane-bound calcium-independent phospholipase A$_2$, *Biochem. Biophys. Res. Commun. 272*, 320−6.
21. Yang, J., Han, X., and Gross, R. W. (2003) Identification of hepatic peroxisomal phospholipase A$_2$ and characterization of arachidonic acid-containing choline glycerophospholipids in hepatic peroxisomes, *FEBS Lett. 546*, 247−50.
22. Mancuso, D. J., Jenkins, C. M., Sims, H. F., Cohen, J. M., Yang, J., and Gross, R. W. (2004) Complex transcriptional and translational regulation of iPLA$_2\gamma$ resulting in multiple gene products containing dual competing sites for mitochondrial or peroxisomal localization, *Eur. J. Biochem. 271*, 4709−24.
23. Van, T. M., Atkins, J., Li, Y., and Glynn, P. (2002) Human neuropathy target esterase catalyzes hydrolysis of membrane lipids, *J. Biol. Chem. 277*, 20942−8.
24. Jenkins, C. M., Mancuso, D. J., Yan, W., Sims, H. F., Gibson, B., and Gross, R. W. (2004) Identification, cloning, expression, and purifications of three novel human calcium-independent phospholipase A$_2$ family members possessing triacylglycerol lipase and acylglycerol transacylase activities, *J. Biol. Chem. 279*, 48968−75.
25. Balsinde, J., Bianco, I. D., Ackerman, E. J., Conde-Friebos, K., and Dennis, E. A. (1995) Inhibition of calcium-independent phospholipase A$_2$ prevents arachidonic acid incorporation and phospholipid remodeling in P388D1 macrophages, *Proc. Natl. Acad. Sci. U.S.A. 92*, 8527−31.
26. Baburina, I., and Jackowski, S. (1999) Cellular responses to excess phospholipid, *J. Biol. Chem. 274*, 9400−8.
27. Larsson, P. K. A., Claesson, H. E., and Kennedy, B. P. (1998) Multiple splice variants of the human calcium-independent phospholipase A$_2$ and their effect on enzyme activity, *J. Biol. Chem. 273*, 207−14.
28. Ma, Z., Wang, X., Nowatzke, W., Ramanadham, S., and Turk, J. (1999) Human pancreatic islets express mRNA species encoding two distinct catalytically active isoforms of group VI phospholipase A$_2$ (iPLA$_2$) that arise from an exon-skipping mechanism of alternative splicing of the transcript from the iPLA$_2$ gene on chromosome 22q13.1, *J. Biol. Chem. 274*, 9607−16.
29. Balboa, M. A., Saez, Y., and Balsinde, J. (2003) Calcium-independent phospholipase A$_2$ is required for lysozyme secretion in U937 promonocytes, *J. Immunol. 170*, 5276−80.
30. Owada, S., Larsson, O., Arkhammar, P., Katz, A. I., Chibalin, A. V., Berggren, P. O., and Bertorello, A. M. (1999) Glucose decreases Na$^+$,K$^+$-ATPase activity in pancreatic β-cells. An effect

mediated via Ca^{2+}-independent phospholipase A_2 and protein kinase C-dependent phosphorylation of the α-subunit, *J. Biol. Chem. 274*, 2000−8.
31. Ramanadham, S., Song, H., Hsu, F. F., Zhang, S., Crankshaw, M., Grant, G., Newgard, C., and Turk, J. (2003) Pancreatic islets and insulinoma cells express a novel isoform of Group VIA phospholipase A_2 (iPLA$_2\beta$) that participates in glucose-stimulated insulin secretion and is not produced by alternate splicing of the iPLA$_2\beta$ transcript, *Biochemistry 42*, 13929−40.
32. Atsumi, G. I., Murakami, M., Kojima, K., Hadano, A., Tajima, M., and Kudo, I. (2000) Distinct roles of two intracellular phospholipase A_2s in fatty acid release in the cell death pathway. Proteolytic fragment of type IVA cytosolic phospholipase $A_2\alpha$ inhibits stimulus-induced arachidonate release, whereas that of type VI Ca^{2+}-independent phospholipase A_2 augments spontaneous fatty acid release, *J. Biol. Chem. 275*, 18248−58.
33. Ramanadham, S., Hsu, F. F., Zhang, S., Jin, C., Bohrer, A., Ma, Z., and Turk, J. (2004) Involvement of the Group VIA Phospholipase A_2 (iPLA$_2\beta$) in endoplasmic reticulum stress-induced apoptosis in insulinoma cells, *Biochemistry 43*, 918−30.
34. Jenkins, C. M., Han, X., Mancuso, D. J., and Gross, R. W. (2002) Identification of calcium-independent phospholipase A$_2\beta$ (iPLA$_2\beta$), and not iPLA$_2\gamma$ as the mediator of arginine vasopressin-induced arachidonic acid release in A-10 smooth muscle cells. Enantioselective mechanism-based discrimination of mammalian iPLA$_2$s, *J. Biol. Chem. 277*, 32807−14.
35. Smani, T., Zakharov, S. I., Csutora, P., Leno, E., Trepakova, E. S., and Bolotina, V. M. (2004) A novel mechanism for the store-operated calcium influx pathway, *Nat. Cell Biol. 6*, 113−20.
36. Williams, S. D., and Ford, D. A. (2001) Calcium-independent phospholipase A_2 mediates CREB phosphorylation and c-fos expression during ischemia, *Am. J. Physiol. 281*, H168−76.
37. Moran, J. M., Butler, R. M., McHowat, J., Turk, J., Wohltmann, M., Gross, R. W., and Corbett, J. A. (2005) Genetic and pharmacologic evidence that iPLA$_2\beta$ regulates virus-induced iNOS expression by macrophages, *J. Biol. Chem. 280*, 28162−8.
38. Murakami, M., Kambe, T., Shimbara, S., and Kudo, I. (1999) Functional coupling between various phospholipase A_2s and cyclooxygenases in immediate and delayed prostanoid biosynthetic pathways, *J. Biol. Chem. 274*, 3103−15.
39. Tay, H. R., and Melendez, A. J. (2004) FcγRI-triggered generation of arachidonic acid and eicosanoids requires iPLA$_2$ but not cPLA$_2$ in human monocytic cells, *J. Biol. Chem. 279*, 22505−13.
40. Ma, Z., Bohrer, A., Wohltmann, M., Ramanadham, S., Hsu, F.-F., and Turk, J. (2001) Studies of phospholipid metabolism, proliferation, and secretion of stably transfected insulinoma cells that overexpress Group VIA phospholipase A_2, *Lipids 36*, 689−700.
41. Bao, S., Bohrer, A., Ramanadham, S., Jin, W., Zhang, S., and Turk, J. (2006) Effects of stable suppression of Group VIA phospholipase A_2 expression on phospholipid content and composition, insulin secretion, and proliferation of INS-1 insulinoma cells, *J. Biol. Chem. 281*, 187−98.
42. Manguikian, A. D., and Barbour, S. E. (2004) Cell cycle dependence of group VIA calcium-independent phospholipase A_2 activity, *J. Biol. Chem. 279*, 52881−92
43. Yellaturu, C. R., and Rao, G. N. (2003) A requirement for calcium-independent phospholipase A_2 in thrombin-induced arachidonic acid release and growth in vascular smooth muscle cells, *J. Biol. Chem. 278*, 43831−7.
44. Roshak, A. K., Capper, E. A., Stevenson, C., Eichman, C., and Marshall, L. A. (2000) Human calcium-independent phospholipase A_2 mediates lymphocyte proliferation, *J. Biol. Chem. 275*, 35692−8.
45. Ramanadham, S., Ma, Z., Arita, H., Zhang, S., and Turk, J. (1998) Type IB secretory phospholipase A_2 is contained in the insulin secretory granules of pancreatic islet β cells and is co-secreted with insulin upon stimulation of islets with glucose, *Biochim. Biophys. Acta 1390*, 301−12.
46. Balsinde, J., and Dennis, E. A. (1996) Bromoenol lactone inhibits magnesium-dependent phosphatidate phosphohydrolase and blocks triacylglycerol biosynthesis in mouse P388D1 macrophages, *J. Biol. Chem. 271*, 31937−41.
47. Fuentes, L., Perez, R., Nieto, M. L., Balsinde, J., and Balboa, M. A. (2003) Bromoenol lactone promotes cell death by a mechanism involving phosphatidate phosphohydrolase-1 rather than calcium-independent phospholipase A_2, *J. Biol. Chem. 278*, 44683−90.
48. Daniels, S. B., Cooner, E., Sofia, M. J., Chakravarty, P. K., and Katzenellenbogen, J. A. (1983) Haloenol lactones. Potent enzyme-activated irreversible inhibitors for α-chymotrypsin, *J. Biol. Chem. 258*, 15046−53.
49. Daniels, S. B., and Katzenellenbogen, J. A. (1986) Halo enol lactones: Studies on the mechanism of inactivation of α-chymotrypsin, *Biochemistry 25*, 1436−44.
50. Song, H., Ramanadham, S., Bao, S., Hsu, F.-F., and Turk, J. (2006) A bromoenol lactone suicide substrate inactivates Group VIA phospholipase A_2 by generating a diffusible bromomethyl ketoacid that alkylates cysteine thiols, *Biochemistry 45*, 1061−73.
51. Paget, M. S. V., and Buttner, M. J. (2003) Thiol-based regulatory switches, *Annu. Rev. Genet. 37*, 91−121.
52. Poole, L. B., Karplus, O. A., and Claiborne, A. (2004) Protein sulfenic acids in redox signaling, *Annu. Rev. Pharmacol. Toxicol. 44*, 325−47.
53. Soberman, R. J. (2003) The expanding network of redox signaling: New observations, complexities, and perspectives, *J. Clin. Invest. 111*, 571−4.
54. Voss, A. A., Lango, J., Ernst-Russell, M., Morin, D., and Pessah, I. N. (2004) Identification of hyperreactive cysteines within ryanodine receptor type I by mass spectrometry, *J. Biol. Chem. 279*, 34514−20.
55. Rhee, S. G., Kang, S. W., Jeong, W., Chang, T. S., Yang, K. S., and Woo, H. A. (2005) Intracellular messenger function of hydrogen peroxide and its regulation by peroxiredoxins, *Curr. Opin. Cell Biol. 17*, 183−9.
56. Geiorgiu, G., and Masip, L. (2003) An overoxidation journey with a return ticket, *Science 300*, 592−4.
57. Wood, Z. A., Poole, L. B., and Karplus, P. A. (2003) Peroxiredoxin evolution and the regulation of hydrogen peroxide signaling, *Science 300*, 650−3.
58. Woo, H. A., Chae, H. Z., Hwang, S. C., Yang, K. S., Kang, S. W., Kim, K., and Rhee, S. G. (2003) Reversing the inactivation of peroxiredoxins caused by cysteine sulfinic acid formation, *Science 300*, 653−6.
59. Nathan, C. (2003) Specificity of a third kind: Reactive oxygen and nitrogen intermediates in cell signaling, *J. Clin. Invest. 111*, 769−78.
60. Palazzolo, A. M., Suquet, C., Konkel, M. E., and Hurst, J. K. (2005) Green fluorescent protein-expressing *Escherichia coli* as a selective probe for HOCl generation within neutrophils, *Biochemistry 44*, 6910−9.
61. Chapman, A. L. P., Hampton, M. B., Senthilmohan, B., Winterbourn, C. C., and Kettle, A. J. (2002) Chlorination of bacterial and neutrophil proteins during phagocytosis and killing of *Staphylococcus aureus*, *J. Biol. Chem. 277*, 9757−62.
62. King, D. A., Hannum, D. M., Qi, J. S., and Hurst, J. K. (2004) HOCl-mediated cell death and metabolic dysfunction in the yeast *Saccharomyces cerevisiae*, *Arch. Biochem. Biophys. 423*, 170−81.
63. Schraufstatter, I. U., Browne, K., Harris, A., Hyslop, P. A., Jackson, J. H., Quehenberger, O., and Cochrane, C. G. (1990) Mechanisms of hypochlorite injury of target cells, *J. Clin. Invest. 85*, 554−62.
64. Vissers, M. C. M., and Winterbourn, C. C. (1995) Oxidation of intracellular glutathione after exposure of human red blood cells to hypochlorous acid, *Biochem. J. 307*, 57−62.
65. Pullar, J. M., Winterbourn, C. C., and Vissers, M. C. M. (1999) Loss of GSH and thiol enzymes in endothelial cells exposed to sublethal concentrations of hypochlorous acid, *Am. J. Physiol. 277*, H1505−12.
66. Pullar, J. M., Vissers, M. C. M., and Winterbourn, C. C. (2001) Glutathione oxidation by hypochlorous acid in endothelial cells produces glutathione sulfonamide as a major product but not glutathione disulfide, *J. Biol. Chem. 276*, 22120−5.
67. Vile, G. F., Rothwell, L. A., and Kettle, A. J. (1998) Hypochlorous acid activates the tumor suppressor protein p53 in cultured human skin fibroblasts, *Arch. Biochem. Biophys. 359*, 51−6.
68. Vissers, M. C. M., Pullar, J. M., and Hampton, M. B. (1999) Hypochlorous acid causes caspase activation and apoptosis or growth arrest in human endothelial cells, *Biochem. J. 344*, 443−9.
69. Midwinter, R. G., Vissers, M. C. M., and Winterbourn, C. C. (2001) Hypochlorous acid stimulation of the mitogen-activated protein kinase pathway enhances cell survival, *Arch. Biochem. Biophys. 394*, 13−20.
70. Green, P. S., Mendez, A. J., Jacob, J. S., Crowley, J. R., Growdon, W., Hyman, B. T., and Heinecke, J. W. (2004) Neuronal expression of myeloperoxidase is increased in Alzheimer's disease, *J. Neurochem. 90*, 724−33.

71. Atouf, F., Czernichow, P., and Scharfmann, R. (1997) Expression of neuronal traits in pancreatic β cells. Implication of neuron-restrictive silencing factor repressor element silencing transcription factor, a neuron-restrictive silencer, *J. Biol. Chem. 272*, 1929−34.
72. Hsu, F.-F., Bohrer, A., and Turk, J. (1998) Electrospray ionization tandem mass spectrometric analysis of sulfatide. Determination of fragmentation patterns and characterization of sulfatide molecular species expressed in brain and pancreatic islets, *Biochim. Biophys. Acta 1392*, 202−16.
73. Robertson, R. P. (2004) Chronic oxidative stress as a central mechanism for glucose toxicity in pancreatic islet β cells in diabetes, *J. Biol. Chem. 279*, 42351−4.
74. Brownlee, M. (2005) The pathobiology of diabetic complications. A unifying mechanism, *Diabetes 54*, 1615−25.
75. Kukidome, D., Nishikawa, T., Sonoda, K., Imoto, K., Fujisawa, K., Yano, M., Motoshima, H., Taguchi, T., Masumura, T., and Araki, E. (2006) Activation of AMP-activated protein kinase reduces hyperglycemia-induced mitochondrial reactive oxygen species production and promotes mitochondrial biogenesis in human umbilical vein endothelial cells, *Diabetes 55*, 120−7.
76. Susztak, K., Raff, A. C., Schiffer, M., and Bottinger, E. P. (2006) Glucose-induced reactive oxygen species cause apoptosis of podocytes and podocyte depletion at the onset of diabetic nephropathy, *Diabetes 55*, 225−33.
77. Fortuno, A., San Jose, G., Moreno, M. U., Beloqui, O., Diez, J., and Zalba, G. (2006) Phagocytic NADPH oxidase overactivity underlies oxidative stress in metabolic syndrome, *Diabetes 56*, 209−15.
78. Ma, Z., Ramanadham, S., Corbett, J., Bohrer, A., Gross, R. W., McDaniel, M. L., and Turk, J. (1996) Interleukin-1 enhances pancreatic islet arachidonic acid 12-lipoxygenase product generation by increasing substrate availability through a nitric oxide-dependent mechanism, *J. Biol. Chem. 271*, 1029−42.
79. Ma, Z., Landt, M., Bohrer, A., Ramanadham, S., Kipnis, D. M., and Turk, J. (1997) Interleukin-1 reduces the glycolytic utilization of glucose by pancreatic islets and reduces glucokinase mRNA content and protein synthesis by a nitric oxide-dependent mechanism, *J. Biol. Chem. 272*, 17827−35.
80. Meyer, M. C., Kell, P. J., Creer, M. H., and McHowat, J. (2005) Calcium-independent phospholipase A_2 is regulated by a novel protein kinase C in human coronary artery endothelial cells, *Am. J. Physiol. 288*, C475−80.
81. Yang, H. C., Mosior, M., Ni, B., and Dennis, E. A. (1999) Regional distribution, ontogeny, purification, and characterization of the Ca^{2+}-independent phospholipase A_2 from rat brain, *J. Neurochem. 73*, 1278−87.
82. Balboa, M. A., Varela-Nieto, I., Killermann, L., Lucas, K., and Dennis, E. A. (2002) Expression and function of phospholipase A_2 in brain, *FEBS Lett. 531*, 12−7.
83. Or, H. K., Fisher, M. T., and Schoneich, C. (2004) Potential role of methionine sulfoxide in the inactivation of eth chaperone GroEL by hypochlorous acid and peroxynitrite, *J. Biol. Chem. 279*, 19486−93.
84. Song, H., Hecimovic, S., Goate, A., Hsu, F. F., Bao, S., Vidavsky, I., Ramanadham, S., and Turk, J. (2004) Characterization of N-terminal processing of group VIA phospholipase A_2 and of potential cleavage sites of amyloid precursor protein constructs by automated identification of signature peptides in LC/MS/MS analyses of proteolytic digests, *J. Am. Soc. Mass Spectrom. 12*, 1780−93.
85. Gross, R. W., Ramanadham, S., Kruszka, K. K., Han, X., and Turk, J. (1993) Rat and human pancreatic islet cells contain a calcium ion independent phospholipase A_2 activity selective for hydrolysis of arachidonate, which is stimulated by adenosine triphosphate and is specifically localized to islet β-cells, *Biochemistry 32*, 327−36.
86. Wang, Z., Ramanadham, S., Ma, Z., Bao, S., Mancuso, D. J., Gross, R. W., and Turk, J. (2005) Group VIA phospholipase A_2 (iPLA$_2\beta$) forms a signaling complex with the calcium/calmodulin-dependent protein kinase IIβ expressed in pancreatic islet β-cells, *J. Biol. Chem. 280*, 6840−9.
87. Bao, S., Jin, C., Zhang, S., Turk, J., Ma, Z., and Ramanadham, S. (2004) Tracking iPLA$_2\beta$ movements in response to stimulation with insulin secretagogues in INS-1 cells, *Diabetes 53*, S186−9.
88. Hampton, M. B., Kettle, A. J., and Winterbourn, C. C. (1998) Inside the neutrophil phagosome: Oxidants, myeloperoxidase, and bacterial killing, *Blood 92*, 3007−17.
89. Brennan, J. P., Wait, R., Begum, S., Bell, J. R., Dunn, M. J., and Eaton, P. (2004) Detection and mapping of widespread intermolecular protein disulfide formation during cardiac oxidative stress using proteomics with diagonal electrophoresis, *J. Biol. Chem. 279*, 41352−60.
90. Marnett, L. J., Riggins, J. N., and West, J. D. (2003) Endogenous generation of reactive oxidants and electrophiles and their reactions with DNA and protein, *J. Clin. Invest. 111*, 583−93.
91. Winterbourn, C. C., and Kettle, A. J. (2000) Biomarkers of myeloperoxidase-derived hypochlorous acid, *Free Radical Biol. Med. 29*, 403−9.
92. Raftery, M. J., Yang, Z., Valenzuela, S. M., and Geczy, C. L. (2001) Novel intra- and inter-molecular sulfinamide bonds in S100A8 produced by hypochlorite oxidation, *J. Biol. Chem. 36*, 33393−401.
93. Chapman, A. L., Winterbourn, C. C., Brennan, S. O., Jordan, T. W., and Kettle, A. J. (2003) Characterization of non-covalent oligomers of proteins treated with hypochlorous acid, *Biochem. J. 1375*, 33−40.
94. Ramanadham, S., Wolf, M. J., Jett, P. A., Gross, R. W., and Turk, J. (1994) Characterization of an ATP-stimulatable Ca^{2+}-independent phospholipase A_2 from clonal insulin-secreting HIT cells and rat pancreatic islets: A possible molecular component of the β-cell fuel sensor, *Biochemistry 33*, 7442−52.
95. Balsinde, J., and Dennis, E. A. (1997) Function and inhibition of intracellular calcium-independent phospholipase A2, *J. Biol. Chem. 272*, 16069−72.
96. Wolf, M. J., and Gross, R. W. (1996) Expression, purification, and kinetic characterization of a recombinant 80-kDa intracellular calcium-independent phospholipase A2, *J. Biol. Chem. 271*, 30879−85.
97. Cumming, R. C., Andon, N. L., Haynes, P. A., Park, M., Fischer, W. H., and Schubert, D. (2004) Protein disulfide bond formation in the cytoplasm during oxidative stress, *J. Biol. Chem. 279*, 21749−58.
98. Claiborne, A., Yeh, J. I., Mallett, T. C., Luba, J., Crane, E. J., III, Charrier, V., and Parsonage, D. (1999) Protein-sulfenic acids: Diverse roles for an unlikely player in enzyme catalysis and redox regulation, *Biochemistry 38*, 15407−16.
99. Denu, J. M., and Tanner, K. G. (1998) Specific and reversible inactivation of protein tyrosine phosphatases by hydrogen peroxide: Evidence for a sulphenic acid intermediate and implications for redox regulation, *Biochemistry 37*, 5633−42.
100. Meng, T. C., Fukada, T., and Tonks, N. K. (2002) Reversible oxidation and inactivation of protein tyrosine phosphatases in vivo, *Mol. Cell 9*, 387−99.
101. Claiborne, A., Mallett, T. C., Yeh, J. I., Luba, J., and Parsonage, D. (2001) Structural, redox, and mechanistic parameters for cysteine-sulfenic acid function in catalysis and regulation, *Adv. Protein Chem. 58*, 215−76.
102. Xanthoudakis, S., Miao, G. G., and Curran, T. (1994) The redox and DNA-repair activities of Ref-1 are encoded by nonoverlapping domains, *Proc. Natl. Acad. Sci. U.S.A. 91*, 23−7.
103. Gorman, M. A., Morera, S., Rothwell, D. G., de La Fortelle, E., Mol, C. D., Tainer, J. A., Hickson, I. D., and Freemont, P. S. (1997) The crystal structure of the human DNA repair endonuclease HAP1 suggests the recognition of extra-helical deoxyribose at DNA abasic sites, *EMBO J. 16*, 6548−58.
104. Rothwell, D. G., Barzilay, G., Gorman, M., Morera, S., Freemont, P., and Hickson, I. D. (1997) The structure and functions of the HAP1/Ref-1 protein, *Oncol. Res. 9*, 275−80.
105. MacCoss, M. J., McDonald, W. H., Saraf, A., Sadygov, R., Clark, J. M., Tasto, J. J., Gould, K. L., Wolters, D., Washburn, M., Weiss, A., Clark, J. I., and Yates, J. R., III (2002) Shotgun identification of protein modifications from protein complexes and lens tissue, *Proc. Natl. Acad. Sci. U.S.A. 99*, 7900−5.
106. Anderson, L. B., Maderia, M., Ouellette, A. J., Putnam-Evans, C., Higgins, L., Krick, T., MacCoss, M. J., Lim, H., Yates, J. R., III, and Barry, B. A. (2002) Posttranslational modifications in the CP43 subunit of photosystem II, *Proc. Natl. Acad. Sci. U.S.A. 99*, 14676−81.
107. Shao, B., Belaaouaj, A., Verlinde, C. L., Fu, X., and Heinecke, J. W. (2005) Methionine sulfoxide and proteolytic cleavage contribute to the inactivation of cathepsin G by hypochlorous acid: An oxidative mechanism for regulation of serine proteinases by myeloperoxidase, *J. Biol. Chem. 280*, 29311−21.

BI060502A